



## RESEARCH & DEVELOPMENT

# Final Report: UAS Roadmap

**Josh Gray, PhD<sup>1,3</sup>**

**Helena Mitasova, PhD<sup>2,3</sup>**

**Rob Austin<sup>4</sup>**

**Gary Blank, PhD<sup>1</sup>**

**<sup>1</sup>Forestry and Environmental Resources**

**<sup>2</sup>Marine, Earth, and Atmospheric Sciences**

**<sup>3</sup>Center for Geospatial Analytics**

**<sup>4</sup>Crop and Soil Sciences**

**NC State University**

**NCDOT Project 2018-01**

**FHWA/NC/2018-01**

**January 2020**

# **Final Report: UAS Roadmap**

**NCDOT #: 2018-01**

Josh Gray, PhD, Helena Mitsova, PhD, Rob Austin, Gary Blank, PhD

**Project Period:** August, 2017 through July, 2019

## TECHNICAL REPORT DOCUMENTATION PAGE

<b>1. Report No.</b> 2008-01	<b>2. Government Accession No.</b>	<b>3. Recipient's Catalog No.</b>	
<b>4. Title and Subtitle</b> Final Report: UAS Roadmap		<b>5. Report Date</b> January 2020	
		<b>6. Performing Organization Code</b>	
<b>7. Author(s)</b> Josh M Gray, PhD Helena Mitsova, PhD Rob Austin Gary Blank		<b>8. Performing Organization Report No.</b>	
<b>9. Performing Organization Name and Address</b> NC State University Center for Geospatial Analytics 2800 Faucette Dr. Campus Box 7106 Raleigh, NC 27695		<b>10. Work Unit No.</b>	
		<b>11. Contract or Grant No.</b>	
<b>12. Sponsoring Agency Name and Address</b> North Carolina Department of Transportation Research and Development Unit 104 Fayetteville Street Raleigh, NC 27601		<b>13. Type of Report and Period Covered</b> Final Report August 2017-July 2019	
		<b>14. Sponsoring Agency Code</b> 2018-01	
<b>15. Supplementary Notes</b> Conducted in cooperation with the U.S. Department of Transportation, Federal Highway Administration.			
<b>16. Abstract</b> We reviewed scientific, technical, and marketplace information relevant to using UAS for mapping wetlands along potential road corridors. This information was synthesized into authoritative guidance on UAS platforms, payloads, flight operations, and the UAS regulatory environment. In particular: 1) UAS scouting can aid in identifying wetland extents when areas are difficult or dangerous to access, 2) very high resolution RGB image mosaics can be created for expert interpretation and to construct extremely detailed terrain models for hyper resolution terrain analysis, and 3) techniques for direct sensing of wetlands with advanced sensors like lidar and radar. Regulatory and technical limitations currently limit the potential of UAS for wetland mapping. Most significantly, beyond line of sight operation is forbidden in most cases, making it difficult to map large areas. When wetlands exist under closed forest canopy, lidar or radar instruments are the only options for direct sensing of the forest floor. But, currently available lidar instruments are expensive, have reduced accuracy compared to traditional systems, require larger aircraft, and are not tightly integrated with the airframe and flight software. The products of this research effort allow NCDOT personnel to compare airframes and payloads, to estimate UAS operational costs, to plan and conduct regulatory compliant UAS flight operations, post-process data into useful forms, and overall: to rapidly and properly scope the potential for integrating UAS into wetland mapping efforts. In doing so, we deliver on the overarching goal articulated in our research contract: to deliver comprehensive, authoritative guidance and implementation strategies for UAS-based remote sensing of wetlands.			
<b>17. Key Words</b> Unmanned aircraft systems, UAS, drones, wetlands, remote sensing, transportation corridors		<b>18. Distribution Statement</b> No restrictions. This document is available through the National Technical Information Service, Springfield, VA 22161.	
<b>19. Security Classif. (of this report)</b> Unclassified	<b>20. Security Classif. (of this page)</b> Unclassified	<b>21. No. of Pages</b> 72	<b>22. Price</b>



## **DISCLAIMER**

The contents of this report reflect the views of the author(s) and not necessarily the views of the University. The author(s) are responsible for the facts and the accuracy of the data presented herein. The contents do not necessarily reflect the official views or policies of either the North Carolina Department of Transportation or the Federal Highway Administration at the time of publication. This report does not constitute a standard, specification, or regulation.

## **Acknowledgments**

The authors are grateful for NCDOT for supporting this research effort. In particular, to Mr. Morgan Weatherford for inspiring and shaping this effort, and to Mr. John Kirby for his patience and guidance. We are indebted to Ms. Justyna Jeziorska for her substantial contributions to this research effort, and to NC State's Center for Geospatial Analytics for institutional support.

## Executive Summary

Collecting data on the presence and extent of wetlands from unmanned aerial systems (UAS) has the potential to improve the efficiency, and reduce the costs of NC DOT's road planning and construction activities. However, the field is emerging and there is rapid development in the UAS scientific, market, and regulatory environments. Thus, there is little focused guidance currently available that would allow UAS-based wetland remote sensing implementation at NC DOT. The overarching goal of the *UAS Roadmap* project was to deliver **comprehensive, authoritative guidance and implementation strategies for UAS-based remote sensing of wetlands**. We envisioned *UAS Roadmap* would proceed in three main phases: knowledge discovery, synthesis, and implementation.

During the project's *Discovery Phase*, a comprehensive survey of the scientific literature was conducted, focusing on UAS remote sensing of wetlands, but including related efforts like sensing inland water bodies, and hydrologic simulation using UAS-derived digital surface models. We summarize the most relevant work in Table 9 of this document, which includes information on their objectives, main findings, UAS platform, and sensor package(s). A thorough review of contemporary marketplace aircraft and sensor package offerings was also conducted. Technical specifications, pricing, and capability information is compiled in a series of tables and figures in this document. Finally, we surveyed the current regulatory environment and provide a thorough overview of current laws, regulations, required licensures, and related compliancy information.

During the project's *Synthesis Phase*, we condensed the vast amount of information from the *Discovery Phase* into a few concrete pathways for including UAS in NC DOT wetland mapping activities. In particular, we highlight roles in simple scouting/surveillance operations that can improve the efficiency and safety of field wetland mapping exercises, using UAS to create extremely accurate, high-resolution digital surface models for hydrologic and/or terrain modeling, and a lidar-specific pathway aimed at solving the problem of detecting wetlands under closed canopy conditions. We also provided a full UAS data collection mission demo from flight planning through final data delivery, fulfilling the objectives of the project's *Implementation Phase*.

The principal limitation in using UAS for NC DOT wetland mapping activities is regulatory: without waivers that are currently extremely difficult to obtain, UAS operation is limited to line-of-sight operation. This severely constricts that size of the ground area that can be efficiently surveyed. Nevertheless, UAS could currently be used over smaller areas to: rapidly visit and verify areas thought/mapped to be wetlands, map the surface conditions under closed canopy with lidar and/or radar sensors, and to update existing digital elevation models with terrain representations at extremely high spatial resolution. Moreover, if future regulations permit beyond-line-of-sight UAS operation, NC DOT could fly small, fixed-wing aircraft with lidar sensors to map the below-canopy surface condition across the entirety of potential road corridors very quickly, and cheaper than a manned aircraft mission.

## Table of Contents

<b>1</b>	<b>INTRODUCTION</b> .....	<b>9</b>
<b>2</b>	<b>BACKGROUND</b> .....	<b>10</b>
<b>3</b>	<b>UAS PLATFORMS</b> .....	<b>12</b>
3.1	THE SYSTEM.....	13
3.2	SENSING PAYLOADS.....	15
3.2.1	..... <i>RGB (visible-band) cameras</i>	16
3.2.2	..... <i>NIR and multispectral cameras</i>	17
3.2.3	..... <i>Hyperspectral Cameras</i>	18
3.2.4	..... <i>Thermal sensors</i>	18
3.2.5	..... <i>Laser scanners</i>	19
<b>4</b>	<b>UAS-BASED SPATIAL DATA</b> .....	<b>20</b>
4.1	DATA ACQUISITION PROCESS.....	20
4.1.1	..... <i>UAS operation and control</i>	20
4.1.2	..... <i>Photogrammetric flight planning</i>	21
4.2	SURFACE RECONSTRUCTION AND STRUCTURE FROM MOTION (SfM).....	24
4.2.1	..... <i>Photogrammetric processing software</i>	25
4.2.2	..... <i>Processing outputs</i>	26
4.3	COST AND TIME EFFECTIVENESS.....	27
4.4	LEGAL CONSTRAINTS.....	29
<b>5</b>	<b>APPLICATIONS FOR WETLAND MAPPING AND HYDROLOGIC MODELING</b> .....	<b>30</b>
<b>6</b>	<b>TABLES</b> .....	<b>32</b>
<b>7</b>	<b>FIGURES</b> .....	<b>42</b>
<b>8</b>	<b>REFERENCES</b> .....	<b>55</b>
<b>9</b>	<b>APPENDIX, SYNTHESIS PATHWAY: SCOUTING</b> .....	<b>63</b>
<b>10</b>	<b>APPENDIX, SYNTHESIS PATHWAY: DSM AND ORTHOPHOTO GENERATION</b> .....	<b>65</b>
<b>11</b>	<b>APPENDIX, SYNTHESIS PATHWAY: LIDAR</b> .....	<b>70</b>

## 1 Introduction

The past decade has seen rapid progress in the miniaturization and affordable production of integrated microelectronics. These developments have made unmanned aircraft systems (UAS) accessible to consumers, and piqued interest in their application to a wide variety of problems. Concurrent advances in sensor technology and data processing have enabled a diverse array of highly accurate measurements to be made with UAS. Regulators have been challenged to keep pace with rapid commercial development and emerging practices, but have responded with clear guidance that preserves a niche for UAS use in commercial and research endeavors. UAS-based solutions have been proposed for almost any conceivable problem, but the greatest impact will be realized for applications that exploit the unique advantages of the technology, namely: work in dangerous or difficult to access areas, high spatial resolution and/or frequent measurements of environmental phenomenon, and deployment of novel sensing technology over small to moderate spatial scales. Collecting spatial data with very high resolution, perhaps frequently, and with unique sensors creates many opportunities for environmental monitoring. Without UAS, most environmental monitoring applications resort to time and resource intensive manual collection of highly detailed information, and/or rely on much coarser scale but more extensive airborne or satellite observations. UAS-based observations offer a middle-ground between these scales of measurement, and so will be most useful when applications require very detailed information of areas too large for manual data collection, but somewhat smaller than is offered by manned aircraft. The identification of jurisdictional wetland areas for road planning purposes is potentially one such application. However, because there is a large and growing assortment of aircraft and sensors available on the market, an evolving regulatory environment, and limited practical guidance or examples of wetland mapping with UAS, it has been difficult to confidently devise or recommend UAS-based monitoring strategies.

This report provides a comprehensive review of UAS hardware, software, regulations, scientific applications, and data collection/post-processing procedures that are relevant for wetland monitoring. Section 2 provides an overview of the wetland mapping problem and

identifies areas that UAS-based observation can provide unique and helpful information. Section 3 provides an overview and technical details for a wide variety of commercially available flight platforms and UAS-mountable sensors. Section 4 gives a detailed account of the UAS data collection procedure including flight planning and post-processing, as well as regulatory information. Finally, Section 5 summarizes the scientific literature on mapping of wetlands from remote sensors and other closely-related topics.

## 2 Background

The challenge in mapping wetlands lies in their delineation from the ground (Madden et al., 2015). The diversity and density of the vegetation as well as the presence of saturated and unstable areas that are impossible to reach by surveyors call for an alternative mapping solution. Therefore, since the advent of aerial photography, in the second half of the 18th century, mapping wetland extents from a “birds’ eye” perspective has been the goal of many aerial surveys. The past several decades have seen a proliferation of imagery from orbital and airborne platforms with a wide range of spatial and spectral resolutions (Belward and Skøien, 2015; Wekerle et al., 2017). Still, the delineation of wetlands has remained challenging. Until recently, there has been a lack of orbital satellites with the ability to produce the very high spatial resolution imagery that might enable the delineation of small wetlands. Even now, with a relatively high number of commercial satellites collecting very high spatial resolution multispectral imagery, the data remain mostly inaccessible due to the high cost, and there have been very few successful wetland mapping efforts (McCabe et al., 2017; Manfreda et al., 2018). Traditional aerial photography from manned aircraft offer an alternative, but this sensing technology is also constrained by cost, operational complexity, and logistical considerations. In terms of spatial scale of measurement and mapping, there has been a void between large to medium sized areas that are the domain of manned aerial surveys, and very small, fine scale terrestrial measurements collected at individual points or for small plots. Advances in unmanned aerial technology promise to fill this gap and provide the types of highly detailed measurements previously only possible with laborious ground measurements, but at much

broader spatial scales. UAS (Unmanned Aerial Systems) provide an alternative platform for capturing data with versatility, adaptability and much greater flexibility than manned airborne systems and satellites, and can offer spatial and spectral resolutions comparable to terrestrial surveys at a fraction of the cost (Pajares, 2015). Additionally, thanks to the ease of use and flexibility of deployment, information can be kept up-to-date more practically and efficiently.

While satellites are still the leading source of large coverage data, UAS are irreplaceable when it comes to affordability and spatial resolution. The ability of UAS to provide sub-inch resolution imagery (and frequently) is unmatched by satellite alternatives. Manfreda et al. (2018) provide a cost comparison between satellite imagery and UAS data. They indicate that satellite provision of high-resolution natural color imagery (50 cm/pix) can cost up to \$3000, whereas UAS not only provide higher resolution (even to couple cm/pix) but for less than \$1000. Unlike satellite or airborne alternatives, the operation of UAS typically requires an initial investment in an UAS platform and the processing software. However, Manfreda et al. (2018) argue that after the purchase, the temporal resolution is limited only by the number of flights (and power supply/battery capacity), so any cost equivalence is quickly overcome due to repeatability. Data storage, man power, field expenses and incidental maintenance are additional, but usually minor costs.

An additional comparison of the cost of data acquisition and processing by UAS, manned aircraft and satellite by Matese et al. (2015) shows that **UAS are the most cost-effective solution for areas 20 ha or smaller**. Their quantitative analyses show that the approximate total cost of a UAS-derived Normalized Difference Vegetation Index (NDVI) map over a 5 ha field is equal to \$450/ha, while similar satellite products may cost about 30% more. Another example of a cost benefit of using UAS can be found in Dustin (2015). The cost of purchasing a UAS platform for the purpose of mapping a park area with an extent of approximately 10 ha is 20% lower than the starting price of hiring a manned aircraft to collect data one time. The cost effectiveness would increase significantly for data collection on a regular basis since the initial

cost of a platform won't contribute to the expenses. More information of the cost and time effectiveness of UAS can be found in section 4.3)

The advantages of UAS for environmental applications such as wetland monitoring go far beyond their cost effectiveness and ability to obtain very high spatial and temporal resolution data. For instance, the rapidity of UAS-based data collection offers near real time spatial information, whereas there is often a lag associated with alternative methods. The flexibility of deployment, especially for the case of rotary-wing UAS solutions (see subsection 3.1), solves a number of accessibility and safety issues in dangerous or hard to reach areas (e.g. in wetlands) (Watts et al., 2012). Although UAS operation depends on weather conditions, van der Wal et al. (2013) calculated that satellite-based remote sensing has a 20% probability of producing an adequate image, while the probability of a usable image from a light-weight, weather sensitive UAS is 45% and rises to over 70% if an all- weather UAS is used. Unlike the sun-synchronous satellite sensors, collecting data with UAS is not limited to certain hours, and with adherence to legal procedures (see section 4.4) enables near continuous environmental monitoring (Manfreda et al., 2018).

These aforementioned capabilities, together with the increasing variety and affordability of UAS and sensor technologies, and the rapid development of processing solutions, have resulted in booming interest in UAS utilization from researchers across various environmental domains.

### 3 UAS Platforms

Remote sensing platforms have been used as a tool for acquiring spatial data even before the invention of the airplane. The need of a bird's-eye view of the Earth surface was pushing the photography pioneers to place cameras in hot air balloons, kites, and even mount them on the breasts of pigeons. With the invention of the airplane, manned airborne aerial photographs started to revolutionize military reconnaissance and surveillance. Analog photographs became the first form of remote sensing used within geography. The next pivotal moment for the development of photogrammetry as a science and technology of making measurements from pictures was the invention of digital photography coupled with advances

in computer science during the last decades of the 20th century. In the same time period UAS technology was widely used in the military context, but its potential for spatial data acquisition was recognized early by geospatial researchers (Przybilla and Wester-Ebbinghaus, 1979). Their early experiments initiated the use of UAS in photogrammetry and remote sensing. 21st century advances in computer science, imaging sensors, autonomous and remote-control techniques, miniaturization of electronic components and the increasing accuracy of global positioning systems (GPS) and inertial measurement units (IMU) paved the way to the rapid development of UAS technology and forever changed the field of photogrammetry and remote sensing, and created endless possibilities for research and business applications. These most recent developments have occurred at an incredible pace, so the intent of this section is to make sense of the wide variety of currently available platforms and sensors that comprise a UAS.

### 3.1 The System

The reader can easily be lost with the multitude of names describing UAS. The media popularized term “drone” can be misleading, pointing out only the flying vehicle itself. Unmanned Aerial Vehicle or UAV, has been used interchangeably with the term UAS, but most recently the latter gained more popularity since including the word system best describes the complexity of the technology. In particular, the term UAS better captures the fact that the aerial vehicle is just one of the components in a much larger system (Fig. 2).

A UAS aircraft’s flight trajectory can be preprogrammed to fly autonomously or manually controlled by a remote pilot. In both cases the ground control station (tablet, laptop, remote control etc.) is a critical component of the system. The data link enabling the communication between aircraft and ground control station is the third essential element of a generic Unmanned Aerial System. Depending on the technology and applications, various UAS models differ not only in size and design but also in included system components. To the most important belong: autopilots, navigating sensors, mechanical steering components, and payloads (typically data acquisition sensors).

The multitude of solutions and systems has invited extensive categorization efforts. Moreover, the diverse and changing nomenclature is amplified by constant innovations and

shifts in technology. The extensive study on UAS typology presented by (Eisenbeiß et al., 2009) covers a variety of classifications, but there is no consistent and commonly accepted scheme of categorizing UAS. Multiple factors (size, weight, flying altitude, endurance, range etc.) and their combinations create endless ways of grouping UAS into categories (see Fig.4). These characteristics influence the payload carrying capacity, as well as operating altitude and range (P'adua et al., 2017). Examples of such classifications can be found in Nex and Remondino (2014), Fahlstrom and Gleason (2012), Austin (2010), Watts et al. (2012) and Zhang and Kovacs (2012). The U.S. Department of Defense has proposed 5 groups (with group 1 having micro and mini subdivisions), presented in 3 and depicted on 4. There is an inconsistency in the naming of these groups (DoD officially uses only numbers), but after Qi et al. (2018) we present the nomenclature commonly used in the field. The use of large (HALE, MALE) and medium sized (tactical) UAS are very restricted (almost exclusively to the military) because of high cost and regulatory burdens. Therefore, the focus of this review is narrowed to systems up to 55 lbs. that can be legally used in the United States for civilian purposes

Recent legislative changes (see: 4.4), coupled with technological advances and miniaturization of electronic components, including the sensors, has precipitated a proliferation in the market of small, lightweight (up to 55 lbs.), off-the-shelf devices that belong to the “micro”, “mini”, or “small UAS” categories. Although their diversity in capabilities and designs is ever increasing, two main types can be recognized: fixed wing and multi-rotor UAS (though hybrid systems do exist).

In the context of hydrological applications and wetland mapping, the initial choice of the type of platform depends on the scope of the particular project. While the nature of the acquired data depends largely on the onboard sensors (described in section 3.2), the platform itself plays a critical role in the success of the remote sensing mission and constrains the types of sensors that may be deployed and flight planning. Fixed wing aircraft have a distinct advantage for wetland mapping because their substantially higher endurance affords the ability to cover much large areas than the average multi-rotor UAS. Fixed wing UAS have been extensively used in land surveying (especially in rural areas), agriculture and environmental management (Senthilnath et al., 2017; Husson et al., 2016; Laliberte et al., 2011). The higher

endurance of fixed wing aircraft is a consequence of their greater aerodynamic efficiency and higher flight speed. In many applications, these characteristics also make the aircraft more stable and allows for greater control over the resulting image quality. Fixed wing UAS have several advantages over the multi rotor UAS (see Tab. 9), but rotary wing (or multi-rotor) aircraft still have distinct applications within wetland mapping.

Rotary wing UAS can be divided into subclasses based on the number of rotor blades. The most common are quadcopters and hexacopters (4 and 6 rotors, respectively). Due to low prices and ease of use, the market of small multi-rotor UAS has boomed in recent years. The relatively shorter endurance of multi-rotor UAS substantially limits the size of the area that can be mapped with one flight. However, multi-rotors have distinct capabilities that may be important in certain contexts: higher payload capacity, ability to remain in one place for a longer time and capture data while hovering, ease of collecting oblique imagery from multiple angles, improved agility and maneuverability that may enable measurements in inaccessible places, and vertical take-off and landing that allows for more flexible deployment and in areas that would be inaccessible with fixed-wing aircraft. Some hybridized solutions offer the aerodynamic advantages of fixed-wing aircraft with the flexibility of VTOL (vertical take-off/landing) or STOL (short take off/landing). While small size fixed wing UAS (e.g. the Sensefly eBee or Quest UAV Datahawk, see: Fig. 3) can be launched from hand, bigger platforms require not only a relatively large take off/landing zone, but also additional launching equipment (e.g. a catapult). We believe these hybrid solutions that combine high endurance and VTOL capability, for example the ARCTURUS JUMP series, with the ability to carry heavy payloads are the future of large scale unmanned aerial mapping. However, the use of such systems for civilian purposes is restricted in most countries, including the U.S., by current legislation (see subsection 4.4).

### 3.2 Sensing Payloads

The optimal combination of carrier and sensing payload is an essential element for obtaining valuable data with UAS-based airborne photogrammetry and remote sensing. While there are an increasing number of fully-integrated platforms available (i.e. aircraft and sensor packages), these typically serve a few specific use cases such as aerial photography and video (equipped with traditional RGB cameras) or thermal inspection. For applications not served by

these integrated offerings, users must carefully consider the pairing of aircraft and sensor. Fitting a remote sensing payload into the weight, volume or mounting restrictions of a specific aircraft is often challenging. Luckily, the availability of a wide variety of UAS-specific sensing payloads has radically increased in recent years. An extensive (but no quite dated) review of advancements in remote sensing instruments can be found in Remondino (2011) and further analysis was published by Colomina and Molina (2014). Here, we aim to summarize the most relevant commercially available UAS sensor offerings for wetland mapping and hydrological modeling. We focus particularly on five types of sensors: visible-band (optical), near-infrared (NIR) and multispectral, hyperspectral, thermal, and laser scanners. While current market sensor offerings are considerable, it is predicted to expand even faster in upcoming years.

Constant improvements enabled by evolutionary advances in miniaturization result in new models appearing on the market each month. It is crucial for a potential buyer to be closely watching those advancements. We expect that this trend will lead to ever smaller, lighter, cheaper, and more capable sensors in the coming years. These advances should increase deployment flexibility because smaller and more affordable UAS systems will be able to carry increasingly sophisticated sensor payloads.

### 3.2.1 RGB (visible-band) cameras

Visible light sensors are capable of capturing imagery perceptible to the human eye. Optical visible light cameras operate in the approximate wavelength range from 400 to 700 nm (Austin, 2010). Since the market of visible range cameras is vast, from mass produced consumer-grade cameras, to professional models, the UAS manufacturers and designers frequently mount existing models on their aircraft. An example of such a solution is the Sony ILCE-QX1 (see Tab. 4 and Fig. 5) mounted on the QuestUAV products.

Since mapping and environmental monitoring is only one of the ranges of UAS applications, it is crucial to know the characteristics of the camera (and the mounting system) to be able to collect useful data. Most of the off-the-shelf drones are equipped with cameras that are used for filming and aerial photography and are not recommended for mapping purposes. However, some of the cameras (like DJI Zenmuse X7, see 4 and Fig. 5) are successfully use in both in the entertainment industry and for mapping missions. In these cases, the most

relevant characteristics of the camera are its image resolution and speed. Many RGB sensors mounted on UAS are capable of providing high-resolution imagery from a bird's eye perspective, as presented in Fig. 6. These types of camera are, by far, the most common and the most affordable monitoring sensors.

These simple cameras realize their environmental mapping and monitoring capabilities through the use of Structure from Motion (SfM) and Multiple View Stereo (MVS) algorithms, described in details in paragraph 4.2. As a result of processing, the RGB imagery can be stitched into orthomosaics (Turner et al., 2016), but can also provide 3D information about the area in form of a 3D mesh, and georeferenced products: point clouds and Digital Surface Models (DSMs) depicted on Fig. 15. Orthophotos and Digital Surface Models are used extensively in wetland monitoring and mapping (more in section 5). The shortcoming of the RGB imagery stems from its very essence – since they capture only the visible spectrum, there is no information about the bare ground under dense vegetation or below canopy line (see Fig. 7). Nevertheless, these cameras serve an important purpose within the context of environmental monitoring, particularly for the creation of high-resolution maps to aid visual interpretation and inspection of difficult to access or dangerous areas.

### 3.2.2 NIR and multispectral cameras

Sensing beyond the visible wavelengths, especially in the near-infrared (NIR) offers unique capabilities, particularly when it comes to the characterization of vegetation (Nebiker et al., 2016). There are multiple UAS-suitable cameras on the market that can capture NIR imagery. Their use is crucial in determining vegetation health (P'adua et al., 2017), and the calculation of a variety of informative spectral indices. Multispectral cameras differ in number of bands, spectral range and resolution. As the sensors become more sophisticated (wider spectral range, more bands), it is more challenging to miniaturize the technology sensor costs rise. Relatively low-cost, off-the-shelf multispectral cameras have been used with success in a wide variety of environmental mapping and monitoring applications (see section 5). Nebiker et al. (2016) compared such a camera with a high end professional UAS dedicated multispectral sensor and found substantial bias and inter-band correlation in the low-cost sensor, but

nevertheless highlighted the practical utility of such sensors for many applications. Some of the more commonly used multispectral cameras are shown in Tab. 5 and on Fig. 8.

### 3.2.3 Hyperspectral Cameras

In spite of the large number of uses of low-cost passive imagery sensors—such as visible (RGB) and near infrared (NIR), many applications require higher spectral fidelity that only multispectral and hyperspectral (Adão et al., 2017) sensors can offer. These sensors acquire images in 10's to 100's of very narrow portions of the electromagnetic spectrum, and so can resolve much subtler spectral variation in targets. Unfortunately, acquisition of such rich data requires sensors that are challenging to miniaturize because of their optics and calibration. Recent hyperspectral technology developments have been consistently resulting in smaller and lighter sensors that can currently be integrated in UAS for either scientific or commercial purposes. Some of them are listed in Tab.6. We believe that such sensors may have a role to play in mapping the locations of particular species, which is not generally possible with coarser spectral resolution measurements, and which may enable wetland identification.

### 3.2.4 Thermal sensors

Although initially used mostly by the military (Kostrzewa et al., 2003), longwave infrared sensors (hereafter: thermal sensors) are now widely used for environmental monitoring. Khanal et al. (2017) reviewed their use in precision agriculture and named applications that are essential also for wetland mapping and monitoring: distribution of soil moisture conditions (Shafian and Maas, 2015; Hassan-Esfahani et al., 2015; Soliman et al., 2013), water stress detection (Osroosh et al., 2015; Gonzalez-Dugo et al., 2013; O'Shaughnessy et al., 2012), soil texture mapping, (Wang et al., 2015) and plant disease detection (Mahlein, 2016; Calderón et al., 2014; Oerke et al., 2010). There is great potential in the use of thermal sensors for the indirect detection and mapping of wetlands. For instance, thermal imagery obtained during times of high vapor pressure deficit and high radiation loads (i.e. bright, dry days) would likely highlight areas that are cooler than their surroundings due to the evaporation of significant water. However, under other meteorological conditions, we might expect that the transpiration of soil water by plants would mask the thermal manifestation of sub-canopy water presence.

### 3.2.5 Laser scanners

With the advent of laser scanning techniques, surveying techniques have been improved by very high quality terrestrial and airborne lidar data (Heritage et al., 2009; Alho et al., 2009; Hodge et al., 2009). Most laser scanners (lidar) employed to characterize topography, bathymetry, and wetlands vegetation are large, heavy, and mounted exclusively on manned aircraft. The market of miniaturized lidar sensors has grown very rapidly and constant technological advancements is improving the quality of data obtained by these sensors. Lang et al. (2015) anticipates that lidar sensor deployment will become more common on UAS. This opens unprecedented opportunity for replacing manned airborne lidar for wetland mapping since the fundamental characteristics of lidar data are largely unaffected by the carrying platform (Lang et al., 2015). This means that well-developed and familiar processing and analytical techniques can be brought to bear on these data sets. The main challenge in UAS lidar application lies in significant trade-offs between performance and the size or cost of the lidar sensor, or the effect of flight dynamics on the measurement process (Wallace et al., 2012). Developing small lidars that can be mounted on UAS necessitates sacrifices in the size, weight and energy source for the lidar (Madden et al., 2015). These limitations typically reduce the effective sensing range of the sensor, but this can be somewhat overcome by the fact that UAS can often fly much closer to the target. The potential of lidar data for wetland extent determination lies in the possibility of obtaining not only the surface information, but also 3D representation of the ground surface underneath (Mitsch and Gosselink, 2007). It has been proven that the use of lidar data yields better accuracy in wetland mapping than photointerpretation – Hogg and Holland (2008) achieved (84%) accuracy in wetland delineation using lidar data compared to CIR images (76%). While the costs of these systems is much higher than other potential payloads, Snyder et al. (2014) shows however a variety of economic benefits that can be achieved by improving topographic maps using lidar that exceeds data acquisition costs. Tab. 8 lists some of the lidar sensors specifically designed for UAS use, some of which are depicted in Fig. 10.

## 4 UAS-based spatial data

This section will focus on describing capabilities and best practices for UAS data acquisition (4.1), raw data processing (4.2), cost and time effectiveness of UAS use (4.3), and the regulatory environment for UAS in the United States (4.4).

### 4.1 Data acquisition process

#### 4.1.1 UAS operation and control

Options for controlling the flight of an unmanned aircraft span a spectrum from complete remote control to fully autonomous flight, with most practical applications employing both to some extent:

- **Ground control:** also known as Remotely Piloted Vehicles (“RPVs”), this control option requires constant input information from an operator. A ground control station (GCS) is a control center located on land or sea that provides aircraft status information (location, orientation, systems information, etc.) and accepts and transmits control information from the operator.
- **Semi-autonomous:** this control method is perhaps the most common and has an operator manually controlling the aircraft during pre-flight, take-off, landing, and a limited set of other maneuvers, but reverts to autopilot enabled autonomous flight for the majority of the mission. For example, the vehicle may be programmed to fly between specified waypoints once in-flight.
- **Fully autonomous:** here control relies on controlling the unmanned vehicle only by the on-board computer without human participation. It means no human input is necessary to perform an objective following the decision to take-off. In this mode, the aircraft must have the capability to assess its condition, and status as well as make decisions affecting its flight and mission.

#### 4.1.2 Photogrammetric flight planning

The mission (flight and data acquisition) is normally planned prior to deployment, off-site, and with the aid of dedicated software. Although available software packages have various interfaces and different mission customization levels, the mapping mission is always defined by indicating the area of interest and geometric flight parameters. Sometimes sensor specifications need to be input manually, but most flight planning platforms have predefined protocols for particular sensor systems, particularly those that are well-integrated with the airframe. In order to plan a successful mapping mission, which ensures the quality of the output data, several principles of traditional photogrammetric flight planning need to be followed.

Longitudinal and transverse overlap of images needs to be maintained (60%-80% in at least one of them, see Fig. 11) and the Ground Sampling Distance (GSD: distance between two consecutive image centers) needs to be determined. The GSD is determined by the flight altitude, focal length, and angle of view of the camera. Geometrical flight parameters vary according to the goal of the flight: missions for detailed mapping require high resolution, high overlap and low flying altitude resulting in small GSDs, but quick flights for emergency surveying and management prioritize flight time at the expense of resolution (Nex and Remondino, 2014). For mapping missions, the autonomous or semi-autonomous mission is generally planned to follow parallel lines and each change of flight trajectory will be marked as a “waypoint”. The image network quality is strongly influenced by the typology of the performed flight (Nex and Remondino, 2014): it is very difficult to ensure the imagery overlap and regular geometry of acquisition in a manual mode, so semi-autonomous operation is most common. Note that these considerations are not unique to the choice of a fixed or rotary wing aircraft, but those choices will imply range and maneuverability constraints that will determine available flight plans.

Flight navigation, but also image orientation for processing purposes, are possible thanks to onboard inertial measurement units (IMU) and GNSS/INS positioning systems. Whether the sensor is fully integrated with the aircraft and navigation electronics or not, measurements (e.g. images) taken by onboard sensors can inherit the geolocation and aircraft attitude information from the navigation unit. This simple “geotagging” solution (see Fig. 12) is ubiquitous, but yields relatively low positional accuracy depending on the quality of the

GNSS/INS position unit, the IMU, and conditions affecting signal strength (e.g. weather). More precise referencing can be achieved with two methods: using Ground Control Points (GCPs) or incorporating Real Time Kinematics (RTK) or Post Processing Kinematics (PPK) devices. The GCP approach relies on post-processing of image mosaics to more accurately georeference them, whereas RTK technology enables more precise positioning at the time of flight/data collection.

### **Ground Control Points (GCPs)**

Ground control points (GCPs) are points on the surface of the Earth of a precisely known location. GCPs are tied in during data processing to georeferenced images from a project and convert ground coordinates of the points to real world locations. They need to be distributed evenly throughout the mapping area before the flight, and measured with high precision techniques such as differential GPS. The precision and accuracy of the data processed with the use of GCPs is very high – on the order of couple of centimeters (Sanz-Ablanedo et al., 2018; Hugenholtz et al., 2016). In the context of wetland mapping and monitoring, the use of GCPs has several shortcomings. First, actually deploying and locating the targets that will serve as GCPs may not be possible in wetland environments due to access issues. Moreover, dense vegetation can make it impossible to identify the targets within the acquired imagery.

### **Real Time Kinematics (RTK) and Post Processing Kinematics (PPK)**

RTK-enabled drones use differential GPS measurements to improve accuracy. The base station (or the Virtual Reference Station – VRS) constantly provides correction and calibration of the UAS position data (see Fig. 13). Each base station measurement is paired in real time with the measurement of the GPS on board the UAS. Successive GPS measurements at the base stations are paired with GPS measurements made by the drone. This provides a mechanism for substantially reducing the errors common between the two measurements (usually resulting in errors on the order of a centimeter or less for the aircraft position relative to the base station). If the UAS operates in the RTK mode, these corrections are applied real-time, requiring an uninterrupted connection between the drone and the base stations throughout the survey. This is hard to achieve in all survey areas, where building, trees, hills can be obstacles in a signal

exchange. This limitation is bypassed by using a Post-Processed Kinematic (PPK) solution, in which the base station and the UAS collect the location data independently and the pairing is executed during the data processing stage. The less accurate data of the GPS onboard the UAS is corrected using the more accurate base station data, resulting in more precise geotags of aerial imagery or other survey data.

Equipment choices (platform, auto-pilot and GCS) fundamentally impact the quality and reliability of the final result: low-cost instruments can be sufficient for small areas, low altitude flights, or in applications with less strict needs for locational precision, while more expensive devices must be used for long endurance flights over wide areas. Generally, in the case of light weight and low-cost platforms, a regular overlap among collected image cannot be ensured due to the strong influence of wind, piloting capabilities and GNSS/INS quality, all randomly affecting the attitude and location of the platforms during the flight. Thus higher overlaps, with respect to flights performed with manned vehicles or very expensive UAVs, are usually necessary to counteract these problems. Wind can greatly affect flight and image acquisition, particularly when interfering with the proper aiming and stability of the sensor system. High winds are not uncommon over coastal wetland areas, and these may impose considerable challenges to flight control and maneuvering. Lighter aircraft and those air frames with larger surfaces tend to be more affected by winds. Recent developments in platform control systems, including improved IMUs, have allowed successful data acquisition campaigns under these challenging scenarios. In addition, the introduction of weatherproof systems has extended data collection capabilities under a variety of environmental conditions. Data acquisition and the quality of the data acquired by a UAS also can be affected by other atmospheric conditions, especially atmospheric effects such as fog and high aerosol concentrations. However, due to the relatively thin atmosphere between the target and the sensor, data derived from UAS are less vulnerable to atmospheric effects than airborne systems flying at higher altitudes. This is a particular advantage for UAS measurements in context where spectral measurement precision is important. While the larger, heavier, more expensive instruments common for orbital or airborne flight often tout much higher spectral calibration accuracies, this may be a moot point when atmospheric correction procedures introduce substantial uncertainty. Therefore, it may

be possible to obtain highly accurate spectral measurements with smaller, cheaper sensors onboard UAS.

#### 4.2 Surface reconstruction and Structure from Motion (SfM)

The concept of combining blocks of aerial images with the aim of creating georeferenced spatial data is a principal of traditional photogrammetry. Traditionally, the key components of the process included generating digital terrain models (DTMs or DEMs) using photogrammetric (Lane et al., 1994; Chandler, 1999; Westaway et al., 2000; Bennett et al., 2012) and differential global positioning system (dGPS) (Brasington et al., 2000) data. As described in section 2 most of these techniques still require expensive equipment and professional knowledge to process data and improve its quality (Micheletti et al., 2015). Development of UAS systems equipped with consumer grade digital cameras provided an opportunity for very low-cost spatial data acquisition. Since the geometry of the photograph is not suitable for measurements, and traditional photogrammetry requires the use of photogrammetric, pre-calibrated cameras, an alternative processing method was needed in order to stitch, georeference and orthorectify the acquired imagery. The computer vision community developed such a method almost 40 years ago: Structure from Motion (SfM) (Ullman et al., 1979) and Multi-View Stereo (MVS) (Seitz et al., 2006), which revolutionized low-cost data acquisition in wetland mapping (Madden et al., 2015) and in other environmental applications (Fonstad et al., 2013; Gomez et al., 2015).

SfM-MVS has the goal of retrieving 3D information from 2D imagery (Gomez et al., 2015). The details of the process have been described by multiple authors (Carrivick et al., 2016; Micheletti et al., 2015; Smith et al., 2015; Fonstad et al., 2013; James and Robson, 2012; Verhoeven et al., 2012; Snavely et al., 2007). The basic principle relies on the identification of common points across a sequence of 2D photographs taken from different angles, and recovering geometric information from the view parallax (Micheletti et al., 2015). Since any particular common point must be present and identified within multiple pictures, it is necessary to have a sufficient overlap between consecutive photographs. The 3D scene consists of a point cloud of these distinct points generated by an automatic feature-detection- and-description algorithm called SIFT (Scale Invariant Feature Transform) (Lowe, 2004). This process results in a scale invariant sparse point cloud (see Fig. 16 B). In order to increase the density of the point

cloud, a conceptual extension of stereo photogrammetry with the use of multiple images (MVS) instead of stereo-pairs, is implemented (Strecha et al., 2008), resulting in the generation of a denser point cloud (see Fig. 16 C). Finally, the dense point cloud can be interpolated into an orthomosaic (using values from vertices colors) and DSM (using the 3D locations, in applied coordinate system). Fig. 16 E and F shows the final result, a DSM and an orthophoto, respectively. There is a critical difference between use of SfM for geomatics applications (i.e. DTM creation) and 3D object modeling. Namely, the need that final image products be georeferenced – placed within a known vertical and horizontal coordinate system (James and Robson, 2012). The method of georeferencing (based on geotags of the photographs, GCPs or using RTK/PPK technology) needs to be determined before the flight mission. Details of this process are described in paragraph 4.1.2. An overview of the strengths and weaknesses of different algorithms used for multi-image SfM is discussed by Smith et al. (2015) and Oliensis (2000), however most commercially available software packages for this purpose utilize procedures optimized for high accuracy and efficiency.

#### 4.2.1 Photogrammetric processing software

The development of SfM algorithms created new possibilities for UAS imagery processing. While the majority of professional photogrammetric software packages, designed initially for processing airborne or satellite imagery, are now able to process UAS imagery, there are distinct advantages for software solutions that are dedicated to UAS image data alone. One of the main strengths of the SfM-MVS approach is its flexibility in the type, number, scale, and positioning of input images that it can handle in the workflow (Carrivick et al., 2016). An additional advantage of SfM algorithms over conventional photogrammetry from stereo-pairs is that in addition to recreating the 3D surface objects or terrain, they recover camera parameters (interior orientation) and positions (exterior orientation). The particular steps of the processing vary based on the software, but the general scheme, based on the SfM-MVS algorithms remains the same. Fig. 15 shows the general pipeline for RGB imagery acquisition and processing.

It is not uncommon that the UAS manufacturer would offer a bundle with flight planning and post-flight imagery processing software (e.g. Trimble provides complete solutions). Advantages of such complete solutions include well-integrated workflows, and technical sup-

port. However, these solutions are often considerably less affordable and have limited flexibility in using alternative aircraft and sensor combinations. Luckily, there is a wide variety of platform-independent software packages, across a range of price points (including free and open source) that allow for flexible and adaptable workflows. The current market

leader is Pix4D (pix4d.com)– who offer a suite of software products that use photogrammetry and computer vision algorithms to transform both RGB and multispectral images into 3D maps and models. Agisoft Metashape (formerly Agisoft Photoscan Professional [www.agisoft.com](http://www.agisoft.com)) is also widely used in a research community. Other proprietary solutions include Bentley ContextCapture), RealityCapture, 3DF Zephyr, Correlator 3D, 3Dsurvey, Menci APS, Autodesk ReCap 360, Icaros OneButton, Drone2Map for ArcGIS + Ortho map- ping in ArcGIS Pro, Trimble Inpho UASMaster, Drone Mapper, Racurs PHOTOMOD UAS and open source solutions: WebODM and MicMac. The software packages differ in price and capabilities. Some them, like Autodesk ReCap Pro or Pix4D Mapper, offer cloud- based processing, which is important when considering the massive computational requirements of SfM-MVS algorithms applied to very large image collections. From standalone licenses, monthly and yearly subscription to pay-by-project solutions, the market of UAS imagery processing software is currently expanding at a hard-to-follow speed. On the other hand, acceptable results can be obtained with a wide variety of packages and the choice should be dictated by budgetary consideration, compute infrastructure, project requirements, integrability with existing workflows and data needs, and the dictates of the chosen aircraft-sensor combination.

#### 4.2.2 Processing outputs

The algorithms described above lead to the creation of multiple geospatial products (see Fig. 16 and blue box on Fig. 15). Primarily, SfM-MVS produces a dense point cloud. The accuracy and precision of which is comparable with point clouds derived from terrestrial or airborne lidar (Wenger, 2016). From this dense point cloud, the following products can be derived:

- **Orthomosaic** – several blending modes (for example assigning a raster color that represents the weighted average value of all pixels from individual photos) can be used for creating a georeferenced orthophotomap. The result looks like an aerial image consisting of all the individual pictures stitched together, but is geometrically correct

and can be used as cartographic material.

- **Digital Surface Model (DSM)** – is created by interpolating the elevation value of the raster cells based on the points that are located within this cell. It is crucial to understand that the product of processing RGB imagery can create a Digital Surface Model, not the bare-earth DEM (see Fig. 7). That is to say, whereas lidar point clouds are often processed to remove canopy returns, that is not possible with DSM.
- **3D Mesh** – is a triangulated irregular network created by connecting the vertices of dense point cloud (see Fig. 16, D) that can also be exported with texture and viewed as colored 3D model.

Orthomosaics and DSMs are crucial products for hydrological modeling and in wetland mapping applications. Terrain representation plays a crucial role in extracting hydrological information (Jenson, 1991) and its accuracy substantially impacts hydrologic predictions (Kenward, 2000). Orthophotos and aerial imagery have been a source for wetland delineation for nearly 50 years (Madden et al., 2015), and are no less useful nowadays. An extended review of the use of the aforementioned spatial data can be found in section 5 of this review.

#### 4.3 Cost and time effectiveness

A comparison of the cost effectiveness of UAS is a challenging endeavor because it invariably fails to account for the many advantages of the UAS data acquisition. That is, while it is possible to compare production costs of very high resolution orthophotos from UAS and airborne systems, such accounting does not reflect the additional value of being able to carry novel sensors, being able to rapidly resurvey a study area, or the value of being able to recover 3D surface information (Manfreda et al., 2018). Nevertheless, several studies have attempted to quantitatively evaluate UAS cost advantages. Carrivick et al. (2016) cast UAS-based Structure from Motion in a broader comparison with traditional surveying methods: total station, dGPS, airborne lidar and traditional photogrammetry (see Fig. 17). Like the UAS, each of these technologies has advantages and disadvantages regarding technological, operational and economic factors (P´adua et al., 2017).

The versatility of the sensors that can be mounted on the UAS make them unique and hard to classify in a cost-effectiveness manner. A separate comparison would need to be made

for each combination of sensor and platform. Bakula et al. (2017) examined the effectiveness of UAS-based lidar for levee monitoring. Thiel and Schmallius (2017) compared photograph based point cloud accuracy with an airborne lidar and observed high match between these two sources, and Wallace et al. (2016) assessed the accuracy in favor of airborne lidar. After a detailed comparison of the cost, time consumption and accuracy of UAS data in comparison to traditional surveying methods, Fitzpatrick (2015) demonstrated that UAS methods cost less, take less time, and Utilizing UAS for data acquisition has three unique advantages:

- low initial investment cost
- low mobilization cost
- decreased time required for data acquisition

In addition to cost and time effectiveness, Manfreda et al. (2018) highlights the UAS ability to collect data in cloudy or hazy conditions that would otherwise obscure satellite retrieval. The low time and resource requirements for UAS deployment make them the most flexible of the data acquisition platforms and provide near real-time capabilities that are required in many environmental applications.

These unprecedented spatiotemporal advantages of UAS do not come without limitations in operations or data processing. These are scrutinized by Whitehead and Hugenholtz (2014) in their review paper. In addition to the already described shortcomings of UAS-collected RGB imagery (variable illumination, irregular resolution due to variable flight altitude, image blur caused by the motion of the platform, etc.), other shortcomings of UAS can be noticed:

- challenges for acquiring and processing data over large spatial scales (legal and technological)
- repeatability depends on factors outside of the control of the surveyor
- more affordable solutions (SfM from RGB sensors, multispectral data) limit the application range

In order to address these shortcomings, best practices in mission and flight planning, sensor configuration, data collection, ground control, image processing and analytics (Manfreda et al., 2018) must be implemented to ensure the final quality of the processed data.

#### 4.4 Legal constraints

The rapid development of UAS technologies in the last couple of decades has resulted in a boom in the drone market, and unmanned vehicles have rapidly populated the airspace. At first, regulatory bodies were applying manned aircraft rules to UAS, but quickly started developing new standards and laws all over the world. In the United States, the Federal Aviation Administration (FAA) introduced, in August 2016, a new set of rules, known as “Part 107” aiming for safe incorporation of UAS into the National Airspace System (Federal Aviation Administration, 2016c). Under this guidance, civilian use is restricted to unmanned vehicles up to 55 lbs. in weight with mandatory registration for those between 0.55 to 55 lbs. The recreational use of drones remains the least regulated, while commercial drone pilots need to obtain a remote pilot certification which requires passing a knowledge test every two years (for those pilots who do not hold at least a manned aircraft sport license). There are important rules restricting in which classes of airspace UAS may be flown (Federal Aviation Administration, 2016a).

With regards to wetland monitoring in particular, and environmental observation in general, important FAA rules constrain the extent of interrogable areas. For instance, the size and flight altitude restrictions (up to 400 ft) limit the area that can be covered by one flight. Furthermore, the UAS operator must maintain visible contact with the aircraft for the flight duration; constituting the biggest obstacle to the mapping of large areas. Although waivers can be granted by FAA which approve certain operations of aircraft outside these limitations (Federal Aviation Administration, 2016b), some of them, like § 107.39 – “Operation Over People” and § 107.31 – “Visual Line of Sight Aircraft Operation” are nearly impossible to obtain. The latter restriction has been the focus of a wide variety of projects aiming to improve unmanned traffic management practices (Jiang et al., 2016) and detect and avoid capabilities (Askelson and Cathey, 2017). The 2018 changes to part § 107.33– “Visual observer” allow for Extended Visual Line of Sight (EVLOS) flights. In EVLOS operations (see Fig. 18), the remote pilot

in command may not have the drone in visible sight at all times, but relies on one or more remote observers to keep the it in visual sight at all times (Federal Aviation Administration, 2018). This development enables more efficient large-scale mapping and mapping within obstacle-rich areas.

## 5 Applications for wetland mapping and hydrologic modeling

The proliferation of UAS technology has impacted a wide-variety of application areas and research domains. In this section, we provide an overview of some of the seminal work on state-of-the-art UAS applications in hydrological modeling and wetland mapping. While most of the analyzed publications concern wetland areas, the review also includes related environmental applications with the strong potential for use in wetland mapping or hydrological modeling. A number of studies have had the specific aim of using UAS to delineate wetlands. Among those, many studies focused on identifying and classifying wetland vegetation using Object-Based Image Analysis (Biggs et al., 2018; Gray et al., 2018; Liu and Abd-Elrahman, 2018; Pande-Chhetri et al., 2017; Husson et al., 2016; Wan et al., 2014). OBIA was discovered to be superior to pixel-based classification by Pande-Chhetri et al. (2017). UAS imagery has also been demonstrated to be suitable for species distribution quick mapping (Li et al., 2017), as well as for training and validating satellite imagery (Gray et al., 2018). Novel techniques for enhancing OBIA have been developed which take advantage of the unique characteristics of UAS data (Liu and Abd-Elrahman, 2018). The versatility of UAS payloads facilitate multi-sensor approaches to environmental monitoring. Sankey et al. (2017) fused data gathered by hyperspectral and lidar sensors obtained by UAS for individual plant species identification and 3D characterization; Wigmore et al. (2019) mapped surface soil moisture in Andean wetlands using thermal and multispectral imagery, and Berni et al. (2009) showed that UAS-based thermal and multispectral imagery yielded comparable estimates to the products of traditional manned airborne sensors.

Those and other UAS uses in hydrological and environmental studies with their respective main objectives and conclusions, as well as the type of the UAS platform and sensor used is compiled in Table 9. While the referenced studies are selective in their application, they

are sufficiently diverse to illustrate many of the major benefits and challenges currently associated with the use of small UAS for wetland mapping and monitoring purposes. They also provide a good snapshot of the present state of the industry. Currently, UAS applications in wetlands are heavily biased towards photogrammetric applications. With the unprecedented pace of platform and sensor development in last decade, it is predicted that the continued evolution will extend the range of wetland related applications for which small UAS are suitable.

## 6 Tables

Table 1: Comparison between different features of fixed-wing and multi-rotor UAS

	<b>Fixed wing</b>	<b>Multi rotor</b>
<b>advantages</b>	<ul style="list-style-type: none"><li>• longer flight autonomy,</li><li>• larger areas covered in less time,</li><li>• better control of flight parameters,</li><li>• higher control of image quality,</li><li>• greater stability (better <u>aerodynamic performance</u><ul style="list-style-type: none"><li>• minor influence of environmental conditions),</li></ul></li><li>• higher flight safety (safer recovery from power loss),</li></ul>	<ul style="list-style-type: none"><li>• greater maneuverability,</li><li>• lower price,</li><li>• more compact and portable,</li><li>• easy to use,</li><li>• higher payload capacity,</li><li>• ability to hover,</li><li>• small landing/takeoff zone</li></ul>
<b>disadvantages</b>	<ul style="list-style-type: none"><li>• <u>less compact</u>,</li><li>• less portable,</li><li>• higher price,</li><li>• challenging to fly</li></ul>	<ul style="list-style-type: none"><li>• shorter range,</li><li>• less stable in the wind,</li></ul>

Table 2: UAS classification (according to Department of Defense), after Qi et al. (2018)

Category	Weight [kg]	Altitude [feet ASL]	Radius [km]	Endurance [hours]
Micro	< 2	up to 200	< 5	< 1
Mini	2–20	up to 3,000	< 25	1–2
Small	20–150	up to 5,000	< 50	1–5
Tactical	150–600	up to 10,000	100 - 300	4–15
MALE	> 600	up to 45,000	> 500	> 24
HALE	> 600	up to 60,000	global	> 24

Table 3: Main relative differences between hyperspectral and multispectral imaging, spectroscopy and RGB imagery, after Adˆao et al. (2017)

	Spectral information	Spatial information
RGBimagery	•	• • •
Multispectral imagery	• •	• • •
Hyperspectral imagery	• • •	• • •
Spectroscopy	• • •	•

Table 4: Main parameters of some commonly used UAS mounted RGB cameras.

Manufacturer and model	Resolution [px]	Weight [g]	speed [ /s]
DJI Zenmuse X7	24 MP (multiple photo sizes)	449	up to 6,000
MAPIR Survey3	4,000×3,000	50*	up to 200
PhaseOne iXU-RS 1000	11,608×8708	930	up to 2,500
Sony ILCE-QX1	5456×3632	158*	up to 4,000
senseFly S.O.D.A.	5,472×3,648	111	up to 2,000

\* without a lens

Table 5: Main parameters of some commonly used multispectral cameras, after Deng et al. (2018), updated.

Manufacturer and model	Resolution [pixels]	Pixel size [ $\mu m$ ]	Weight [g]	Spectral range Central wavelength [nm] (Band with [nm])
Buzzard Camera six	1,280×1,024	5.3	250	Blue: 500 (50) Green: 550 (25) Red: 675 (25) NIR1: 700 (10) NIR2: 750 (10) NIR3: 780 (10)
MicaSense RedEdge	1,280×960	3.75	180	Blue: 475 (20) Green: 560 (20) Red: 668 (10) Red edge: 717 (10) NIR: 840 (40)
Parrot Sequoia+	1,280×960	3.75	71	Green: 550 (40) Red: 660 (40) Red edge: 735 (10) NIR: 790 (40)
Senterra Quad	1,248×950	3750	0.17	RGB Red: 655 (40) Red edge: 725 (25) NIR: 800 (25)
Tetracam ADC Micro	2,048×1,536	3200	0.09	Green: 520–600 Red: 630–690 NIR: 760–900
Tetracam MiniMCA6	1,280×1,024	5.2	700	Blue: 490 (10) Green: 550 (10) Red: 680 (10) Red edge: 720 (10) NIR1: 800 (10) NIR2: 900(20)

Table 6: Main parameters of some hyperspectral sensors available for being coupled with UAS, modified from Adão et al. (2017)

Manufacturer and model	Spectral range [nm]	Number of bands	Spatial resolution [px]	Weight [g]
BaySpec OCI-UAV-1000	600–1000	100	2048*	272
Brandywine Photonics CHAI V-640	350–1080	256	640×512	480
HySpex VNIR-1024	400–1000	108	1024*	4000
NovaSol Alpha-SWIR microHSI	900–1700	160	640*	1200
Quest Hyperea 660 C1	400–1000	660	1024*	1440
Resonon Pika L	400–1000	281	900*	600
Resonon Pika NIR	900–1700	164	320*	2700
SENOP VIS-VNIR Snapshot	400–900	380	1010×1010	720
SPECIM SPECIM FX17	900–1700	224	640*	1700
Surface Optics Corp. SOC710-GX	400–1000	120	640*	1250
XIMEA MQ022HG-IM-LS150-VISNIR	470–900	150+	2048×5	300

\* Pushbroom length line

Table 7: Some of the currently available thermal cameras, after Khanal et al. (2017), modified.

Manufacturer and model	Resolution [px]	Weight [g]	Spectral band [ $\mu\text{m}$ ]
FLIR T450sc	320x240	880*	7.5–13.0
FLIR Tau 640	640x512	110	7.5–13.5
FLIR Thermovision A40M	320x240	1400	7.5–13.5
ICI 320x	320x240	150*	7.0–14.0
ICI 7640 P-Series	640x480	127.6	7.0–14.0
InfraTec mobileIR M4	160x120	265*	8.0–14.0
Optris PI400	382x288	320*	7.5–13.0
Pearleye LWIR	640x480	790*	8.0–14.0
Photon 320	324x256	97	7.5–13.5
Tamarisk 640	640x480	121	8.0–14.0
Thermoteknix MIRICLE 370 K	640x480	166	8.0–12.0
Xenix Gobi-384 (Scientific)	384x288	500*	8.0–14.0

\*with housing and lens

Table 8: Main parameters of some lidar sensors designed for UAS

Manufacturer and model	Range [m]	Weight [g]	Field of view[°]	Laser class	Accuracy [mm]
Riegl VUX-1UAV	3–350	3500	330	1	10
Riegl VUX-240	5–1400	3800	$\pm 37.5$	3R	20
Routescene UAV LidarPod	0–100	1300	(H)41, (V)360	1	(XY) 15* (Z) 8*
Velodyne HDL-32E	80–100	1300	(H)360, (V)+10 to -30	1	20
Velodyne PUC VLP-16	0–100	830	(H)360, (V) $\pm 15$	1	30
YellowScan Mapper II	10–75	2100	100	1	(XY) 150 (Z) 50
YellowScan Surveyor	10–60	1600	360	1	50

(G) Horizontal  
(V) Vertical

\*with RTK

Table 9: Compilation of hydrological and environmental studies presenting their respective main objectives and conclusions and UAS type and sensors used in each case. **F** - fixed wing, **R** - rotary wing, **V** - visible range, **T** - thermal, **M** - multispectral, **H** - hyperspectral, **L** - lidar

Reference	Objective	Main conclusion	Type		Sensor used				
			F	R	V	T	M	H	L
Wigmore et al. (2019)	Map surface soil moisture content in Andean wetlands using UAS based multispectral imagery to better understand controls and impacts on its observed spatial variability within these systems.	UAS can provide reliable sub-metre estimates of surface soil moisture and provide unique insights into spatially heterogeneous environments.		R		T	M		
Biggs et al. (2018)	Coupling UAS and hydraulic surveys to study the geometry and spatial distribution of aquatic macrophytes	The aerial surveying techniques can be used to efficiently estimate vegetation abundance, surface area blockage factor and also to visualise flow through patch mosaics, enabling targeted management of aquatic vegetation.		R		V			
Gray et al. (2018)	Classification of estuarine wetlands based on WorldView-3 and RapidEye satellite imagery, using UAS imagery to assist training a Support Vector Machine.	UAS can be highly effective in training and validating satellite imagery. Within a fixed budget, it allows much larger training and testing sample sizes. The UAS accuracy is similar to field-based assessments.	F			V			

Table 9: Compilation of hydrological and environmental studies presenting their respective main objectives and conclusions and UAS type and sensors used in each case. **F** - fixed wing, **R** - rotary wing, **V** - visible range, **T** - thermal, **M** - multispectral, **H** - hyperspectral, **L** - lidar

Reference	Objective	Main conclusion	UAS		Sensor used				
			F	R	V	T	M	H	L
Liu and Abd-Elrahman (2018)	Testing approach seamlessly integrating multi-view data and object-based classification of wetland land covers.	Multi-view OBIA (MV-OBIA) substantially improves the overall accuracy compared with traditional OBIA, regardless of the features used for classification and types of wetland land covers. Two window-based implementations of MV-OBIA both show potential in generating an equal if not higher overall accuracy compared with MV-OBIA at substantially reduced computational costs.	✓		V				
Sankey et al. (2017)	A fusion method for individual plant species identification and 3D characterization at submeter scales based on UAV lidar and hyperspectral imagery.	UAS lidar characterized the individual vegetation canopy structure and bare ground elevation, whereas the hyperspectral sensor provided species-specific spectral signatures for the dominant and target species at study area. The fusion of the two different data sources performed better than either data type alone in the arid and semi-arid ecosystems with sparse vegetation.		R				H	L
Li et al. (2017)	Assess the utility of UAV-borne hyperspectral image and photogrammetry derived 3D data for wetland species distribution quick mapping	The utility of UAV-borne hyperspectral and photogrammetry-derived 3D data help to characterize and monitor wetland environment. UAS offers a solution for detail species survey of wetland area in relatively low cost of time and labor.		R	V			H	

Table 9: Compilation of hydrological and environmental studies presenting their respective main objectives and conclusions and UAS type and sensors used in each case. **F** - fixed wing, **R** - rotary wing, **V** - visible range, **T** - thermal, **M** - multispectral, **H** - hyperspectral, **L** - lidar

Reference	Objective	Main conclusion	UAS		Sensor used			
			F	R	V	T	M	H
Pande-Chhetri et al. (2017)	Comparison of classification methods for wetland vegetation based on UAS imagery.	The use of OBIA of high spatial resolution (sub-decimeter) UAS imagery is viable for wetland vegetation mapping. Object-based classification produced higher accuracy than pixel-based classification. Disadvantage for OBIA is a great amount of time and efforts spent on scale parameter selection or post-classification refinement for an object-based approach with expert knowledge.	F		V			H
Senthilnath et al. (2017)	Evaluation of performance of proposed spectral-spatial classification methods for crop region mapping and tree crown mapping of images acquired using UAV.	UAV images obtained using the two UAV platforms were used to demonstrate the performance of the proposed algorithm. From the obtained results, it was concluded that the proposed spectral-spatial classification performs better and was more robust than the other algorithms in the literature.	F	R	V			
Boon et al. (2016)	Assess if the use of UAV photogrammetry can be used to enhance the wetland delineation classification and WET-Health assessment	UAV photogrammetry can significantly enhance wetland delineation and classification but also be a valuable contribution to WET-Health assessment		R	V			
Husson et al. (2016)	Comparison of Manual Mapping and Automated Object-Based Image Analysis of Non-Submerged Aquatic Vegetation	Automated classification of non-submerged aquatic vegetation from true-colour UAS images was feasible, indicating good potential for operative mapping of aquatic vegetation.	F		V			

Table 9: Compilation of hydrological and environmental studies presenting their respective main objectives and conclusions and UAS type and sensors used in each case. **F** - fixed wing, **R** - rotary wing, **V** - visible range, **T** - thermal, **M** - multispectral, **H** - hyperspectral, **L** - lidar

Reference	Objective	Main conclusion	UAS		Sensor used				
			F	R	V	T	M	H	L
Wallace et al. (2016)	Investigation of the potential of UAS based airborne laser scanning and structure from motion (SfM) to measure and monitor structural properties of forests.	Although ALS is capable of providing more accurate estimates of the vertical structure of forests across the larger range of canopy densities found in this study, SfM was still found to be an adequate low-cost alternative for surveying of forest stands.		R	V				L
Tamminga et al. (2014)	Assess the capabilities of an UAS to characterize the channel morphology and hydraulic habitat with the goal of identifying its advantages and challenges for river research and management	By enabling dynamic linkages between geomorphic processes and aquatic habitat to be established, the advantages of UAVs make them ideally suited to river research and management.		R	V				
Wan et al. (2014)	Monitoring the invasion of <i>Spartina alterniflora</i> using very high resolution UAS imagery	Imagery can provide details on distribution, progress, and early detection of <i>Spartina alterniflora</i> invasion. OBIA, object based image analysis for remote sensing detection method, can enable control measures to be more effective, accurate, and less expensive than a field survey.		R	V				H
Zarco-Tejada et al. (2012)	Detect water stress based on Fluorescence, temperature and narrow-band indices acquired from a UAV platform	The research proves feasibility of thermal, narrow-band indices and fluorescence retrievals obtained from a micro-hyperspectral imagery and a light-weight thermal camera on board small UAV platforms for stress detection in a heterogeneous tree canopy where very high resolution is required.	F			T			H

Table 9: Compilation of hydrological and environmental studies presenting their respective main objectives and conclusions and UAS type and sensors used in each case. **F** - fixed wing, **R** - rotary wing, **V** - visible range, **T** - thermal, **M** - multispectral, **H** - hyperspectral, **L** - lidar

Reference	Objective	Main conclusion	UAS		Sensor used				
			F	R	V	T	M	H	L
Laliberte et al. (2011)	Develop a relatively automated and efficient image processing workflow for deriving geometrically and radiometrically corrected multispectral imagery from a UAS for the purpose of species-level rangeland vegetation mapping	Comparison of vegetation and soil spectral responses for the airborne and WorldView-2 satellite data demonstrate potential for conducting multi-scale studies and evaluating upscaling the UAS data to larger areas.	F						M
Berni et al. (2009)	Generate quantitative remote sensing products by means of an UAS equipped with inexpensive thermal and narrow-band multispectral imaging sensors and compare them to the products of traditional manned airborne sensors.	The low cost and operational flexibility, along with the high spatial, spectral, and temporal resolutions provided at high turnaround times, make this platform suitable for a number of applications, where time-critical management is required. The results yielded comparable estimations, if not better, than those obtained by traditional manned airborne sensors.		R			T	M	

## 7 Figures

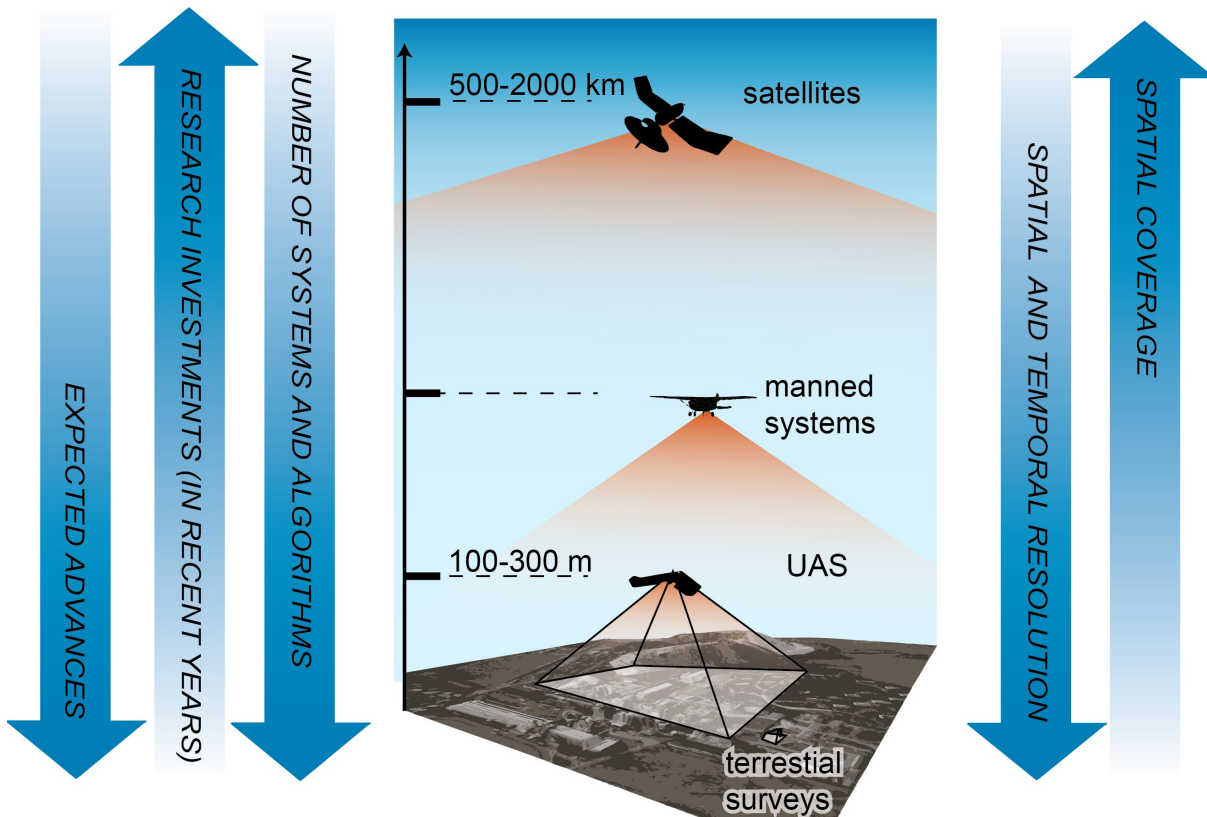


Figure 1: Comparison of the most important aspects of spatial data acquisition, after

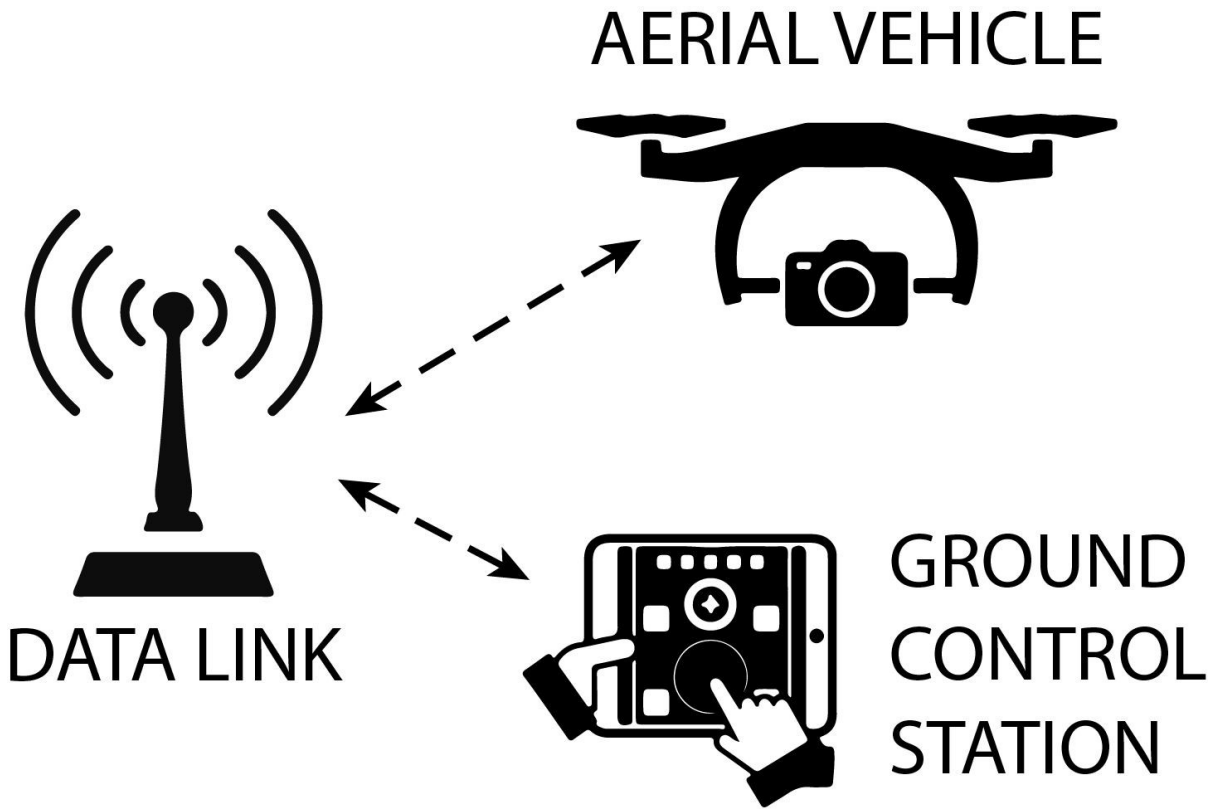


Figure 2: Architecture of Unmanned Aerial System

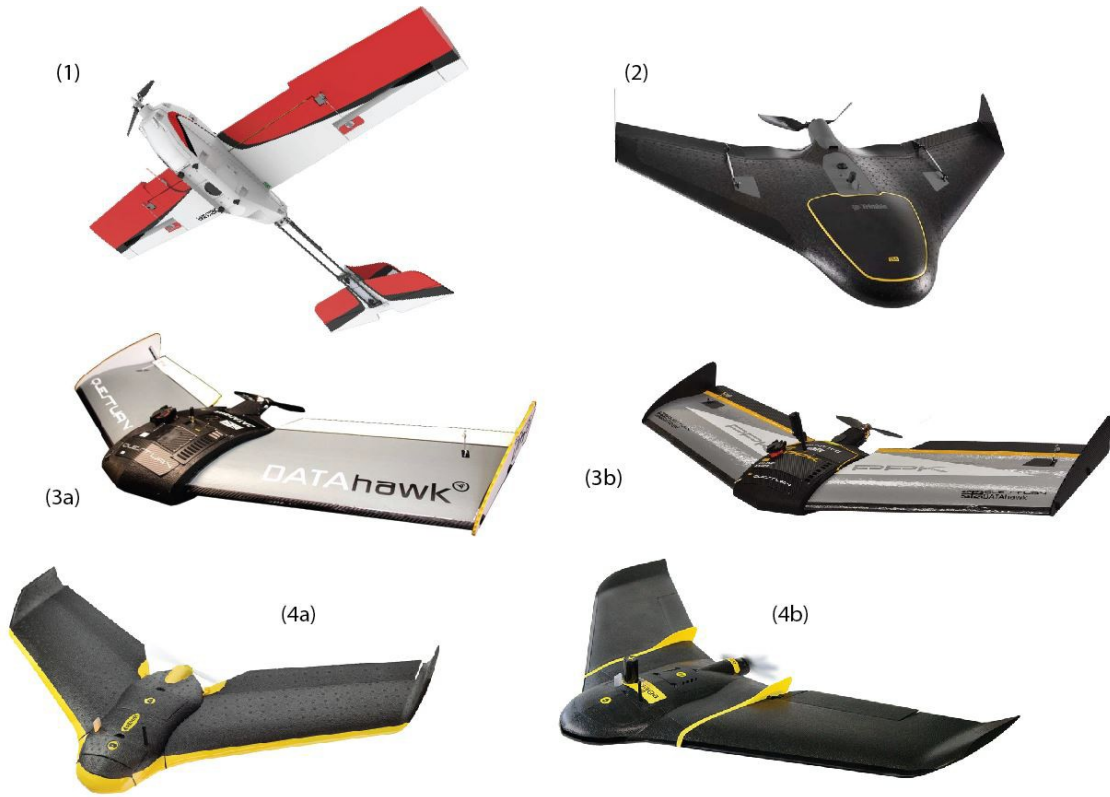


Figure 3: Examples of fixed wing UAS (1) Precision Hawk Lancaster 5 (2) Trimble UX5 (3a) QuestUAV DATAhawk (3b) QuestUAV DATAhawk PPK (4a) senseFly eBee (4b) senseFly eBee Plus

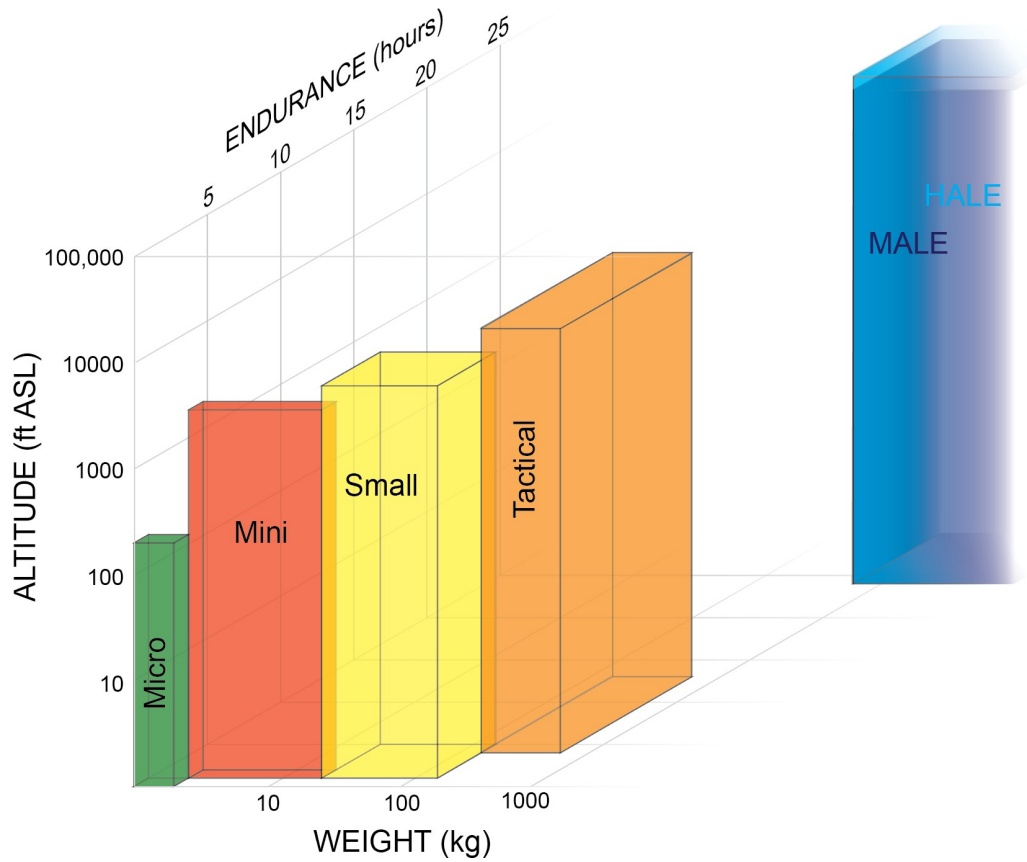


Figure 4: DoD UAS Classifications



Figure 5: Some commonly used UAS RGB cameras, listed in Tab. 4: (A) DJI Zenmuse X7, (B) MAPIR Survey3 (also available in multispectral option), (C) PhaseOne iXU-RS 1000, (D) Sony ILCE-QX1, (E) senseFly S.O.D.A. Images not to scale



Figure 6: An RGB imagery of wetland area captured by Sony NEX-5T camera mounted on Trimble UX5 (see Fig. 3). Flight altitude – 135 m, data captured 02/17/2017.

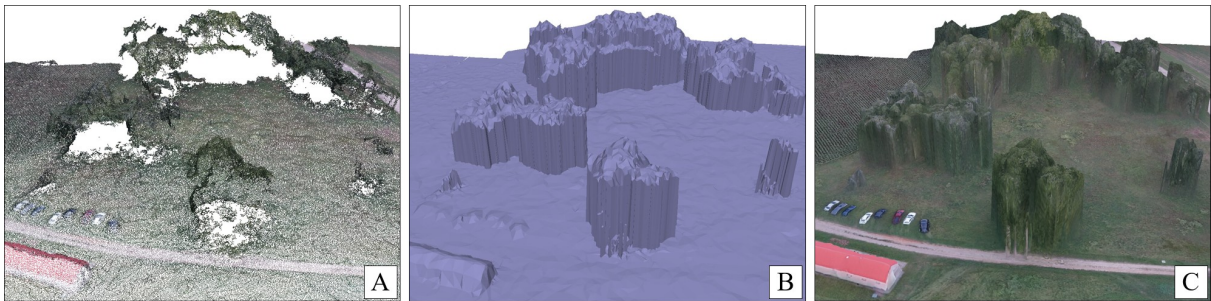


Figure 7: Processed RGB imagery using SfM techniques. Visible lack of data below the canopy on dense point cloud (A) and resulting misrepresentation of the canopy structure on 3D model (B) and textured 3D model (C).



Figure 8: Some commonly used UAS multispectral cameras: (A) Buzzard Camera six, (B) MicaSense RedEdge, (C) Parrot Sequoia+, (D) Sentera Quad, (E) Tetracam ACD Micro, (F) Tetracam MiniMCA6. Images not to scale



Figure 9: Some commonly used UAS multispectral cameras: (A) Buzzard Camera six, (B) MicaSense RedEdge, (C) Parrot Sequoia+, (D) Sentera Quad, (E) Tetracam ACD Micro, (F) Tetracam MiniMCA6. Images not to scale



Figure 10: Some commonly used lidar sensors for UAS, listed in Tab.8: (A) Riegl VUX-1UAV, (B) Riegl VUX-240, (C) Rousescene UAV LidarPod, (D) Velodyne HDL-32E, (E) Velodyne PUC VLP-16, (F) YellowScan Mapper II, (G) YellowScan Surveyor.

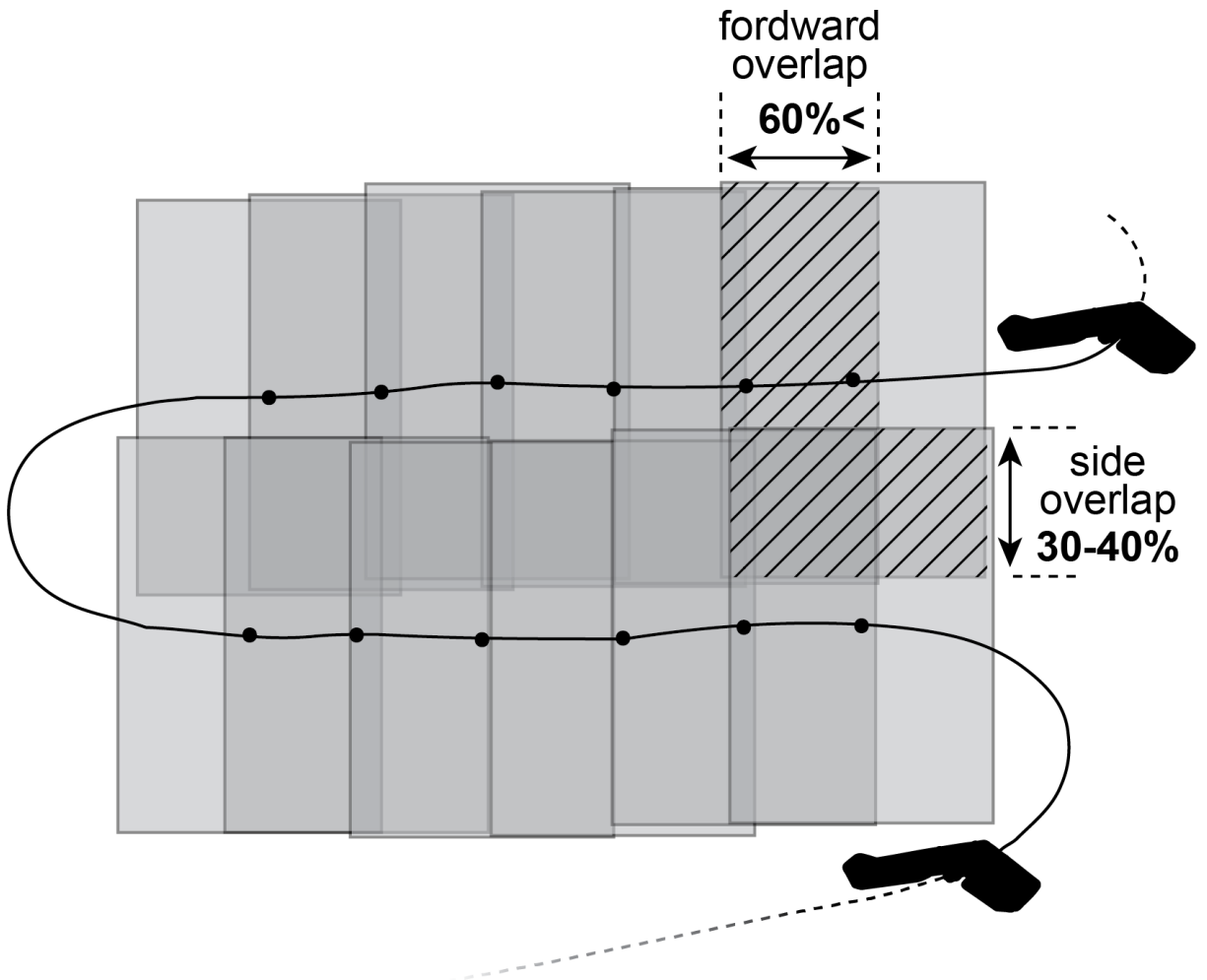


Figure 11: Schematic overview of photogrammetric UAS flight

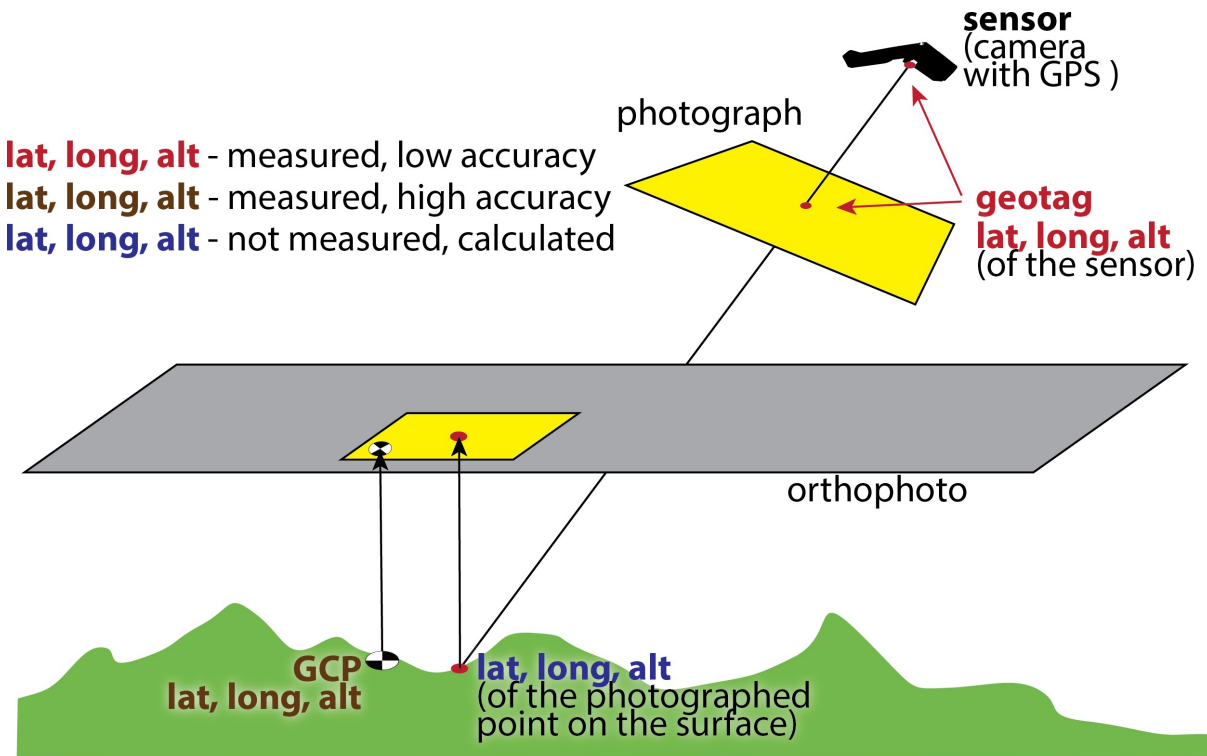


Figure 12: Comparison of georeferencing based on GCPs and imagery geotags.

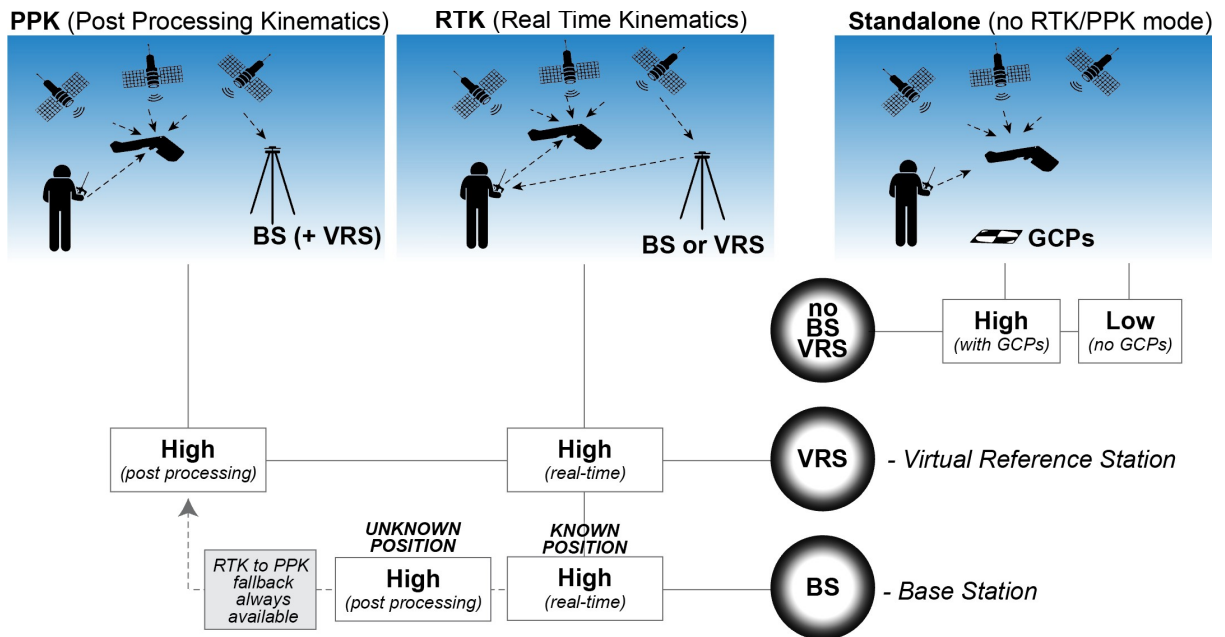


Figure 13: Achievable absolute accuracy using Real Time Kinematics or Post Processing Kinematics-enabled and Standalone UAS

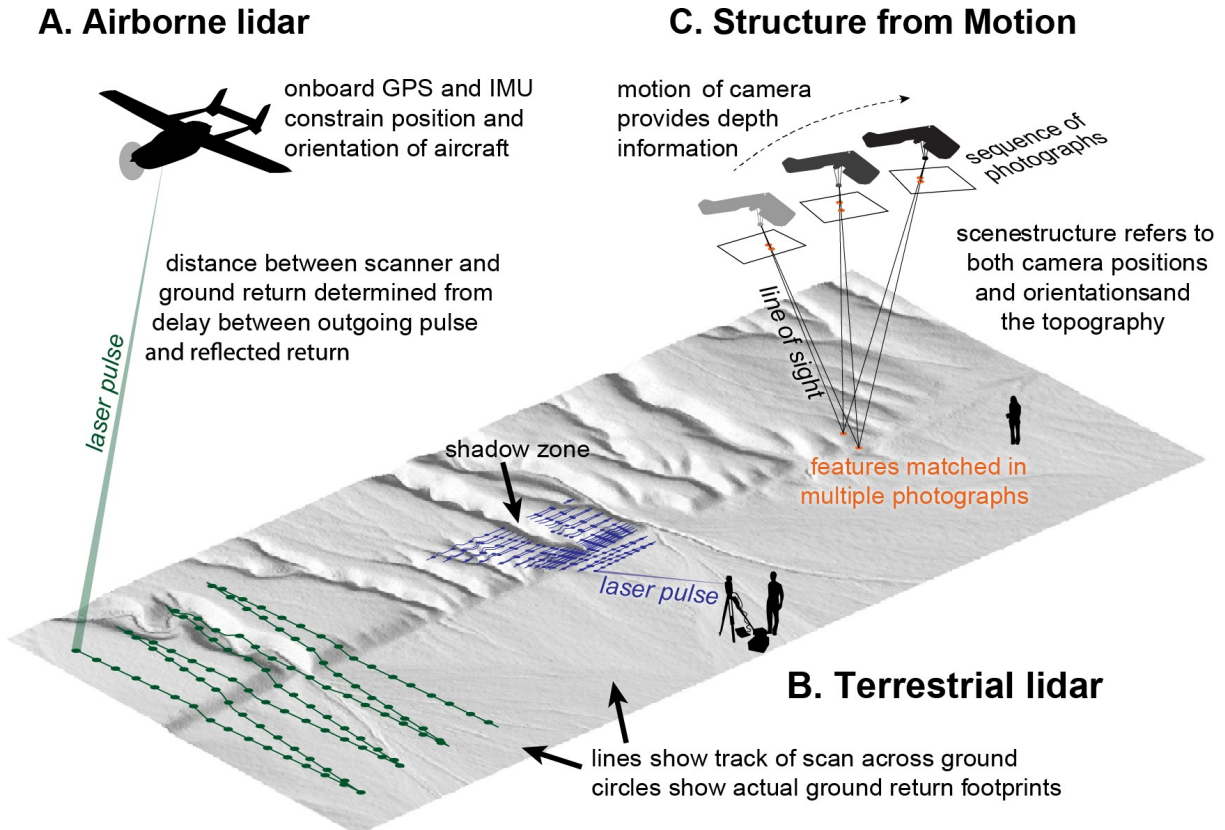


Figure 9: A schematic illustration of three methods of producing high-resolution digital topography: A. Airborne lidar (light detection and ranging), B. Terrestrial lidar, C. UAS-based structure from Motion (GPS – global positioning system; IMU – inertial measurement unit), modified from (Johnson et al., 2014).

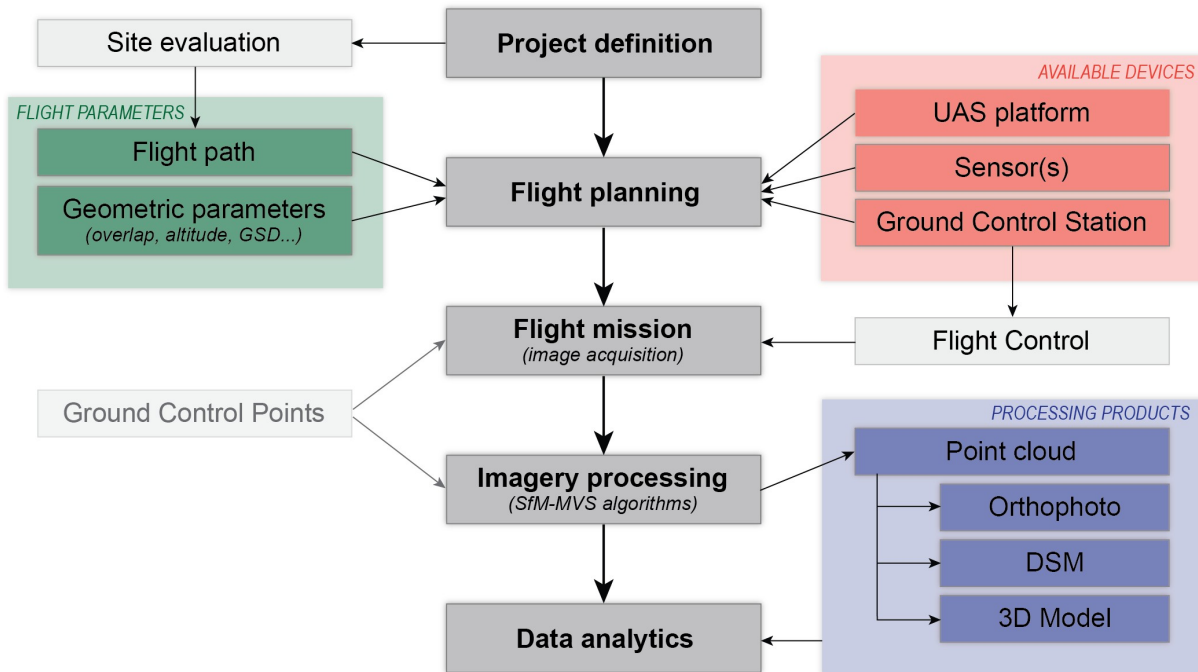


Figure 10: Typical acquisition and processing pipeline for RGB imagery with the use of SfM-MVS algorithms

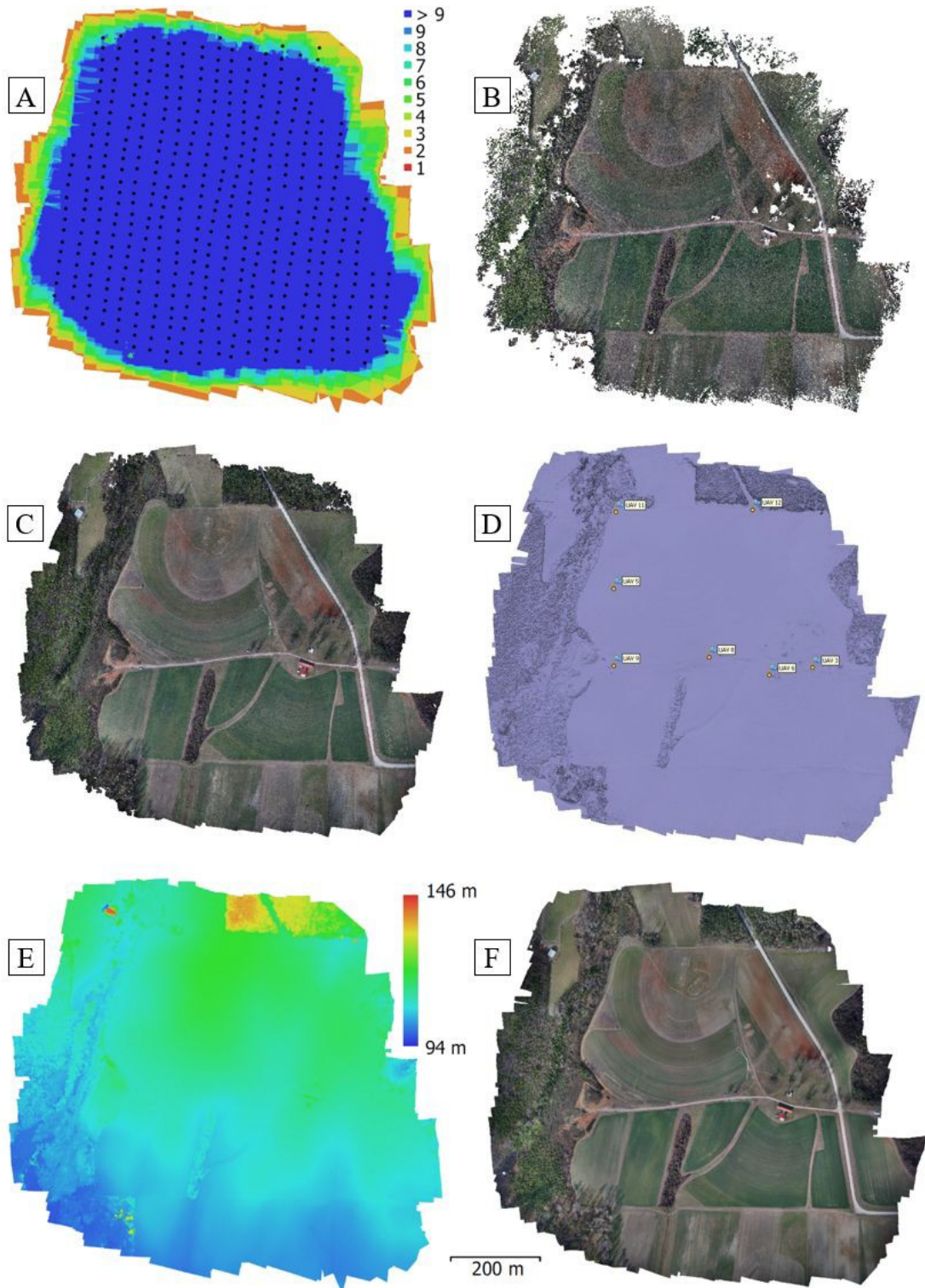


Figure 11: An example UAS image processing workflow. (A) Photo capturing positions and image overlap (B) Sparse point cloud (C) Dense point cloud (D) Mesh with indicated positions of Ground Control Points (E) DSM (F) Orthomosaic

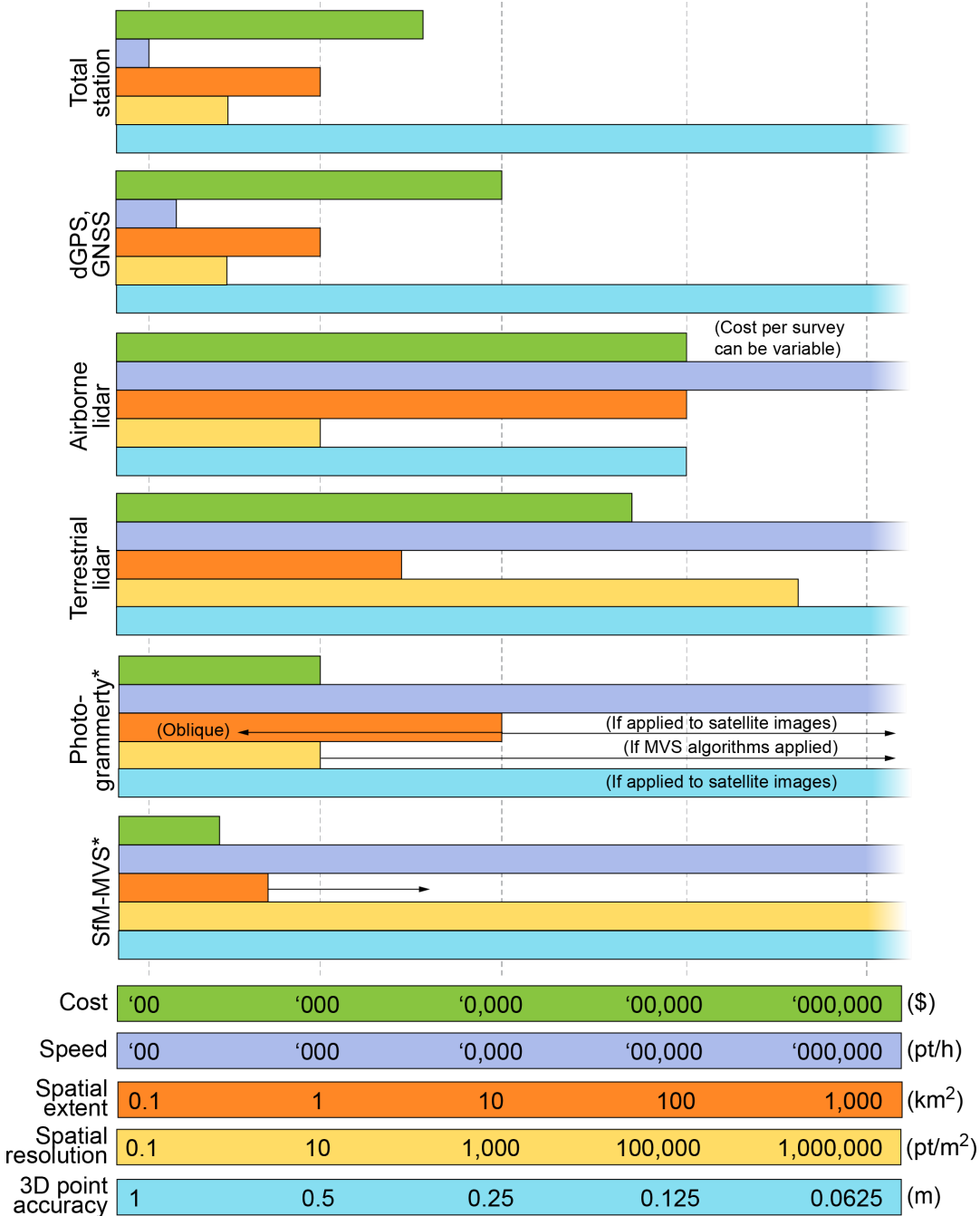


Figure 12: Comparison of digital survey methods with regard to financial cost, maximum possible speed, spatial coverage, resolution, and accuracy; after Fig. 2.7 in Carrivick et al. (2016)

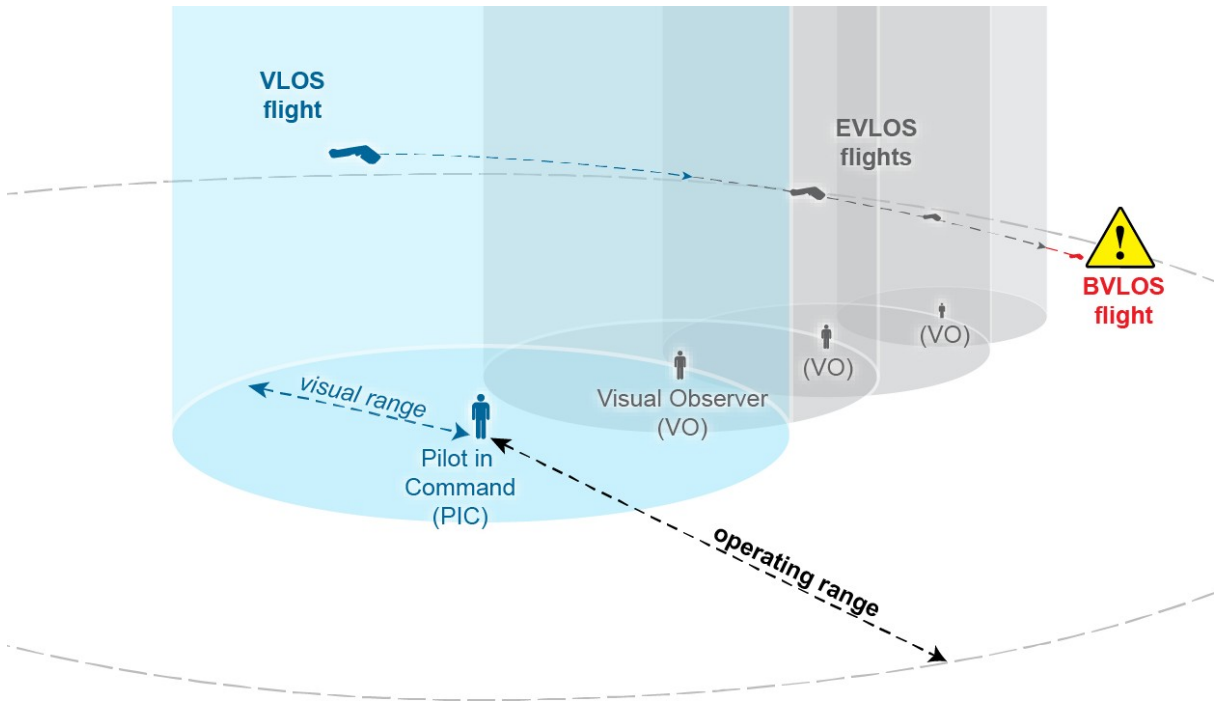


Figure 13: Flights in the visual range (VLOS), extended visual line of sight (EVLOS) and beyond visual line of sight (BVLOS)

## 8 References

- Adão, T., Hruška, J., Pádua, L., Bessa, J., Peres, E., Morais, R., Sousa, J., 2017. Hyperspectral imaging: A review on UAV-based sensors, data processing and applications for agriculture and forestry. *Remote Sensing* 9 (11), 1110.
- Alho, P., Kukko, A., Hyypä, H., Kaartinen, H., Hyypä, J., Jaakkola, A., 2009. Application of boat-based laser scanning for river survey. *Earth Surface Processes and Landforms* 34 (13), 1831–1838.
- Askelson, M., Cathey, H., 2017. Small UAS Detect and Avoid Requirements Necessary for Limited Beyond Visual Line of Sight (BVLOS) Operations. Tech. rep.
- Austin, R., 2010. Unmanned aircraft systems : UAVs design, development and deployment. Wiley, Chichester.
- Bakuła, K., Salach, A., Wziatek, D. Z., Ostrowski, W., Górski, K., Kurczynski, Z., 2017. Evaluation of the accuracy of lidar data acquired using a UAS for levee monitoring: preliminary results. *International Journal of Remote Sensing* 38 (8-10), 2921–2937.
- Belward, A. S., Skøien, J. O., 2015. Who launched what, when and why; trends in global land-cover observation capacity from civilian earth observation satellites. *ISPRS Journal of Photogrammetry and Remote Sensing* 103, 115 – 128, global Land Cover Mapping and Monitoring.
- Bennett, G., Molnar, P., Eisenbeiss, H., McArdell, B., 2012. Erosional power in the swiss alps: characterization of slope failure in the illgraben. *Earth Surface Processes and Landforms* 37 (15), 1627–1640.
- Berni, J. A. J., Zarco-Tejada, P. J., Suarez, L., Fereres, E., 2009. Thermal and narrowband multispectral remote sensing for vegetation monitoring from an unmanned aerial vehicle. *IEEE Transactions on Geoscience and Remote Sensing* 47 (3), 722–738.
- Biggs, H. J., Nikora, V. I., Gibbins, C. N., Fraser, S., Green, D. R., Papadopoulos, K., Hicks, D. M., 2018. Coupling unmanned aerial vehicle (uav) and hydraulic surveys to study the geometry and spatial distribution of aquatic macrophytes. *Journal of Ecohydraulics* 3 (1), 45–58.
- Boon, M. A., Greenfield, R., Tesfamichael, S., 2016. Wetland assessment using unmanned aerial vehicle (UAV) photogrammetry. *International Archives of the Photogrammetry, Remote Sensing and Spatial Information Sciences - ISPRS Archives* 41, 781–788.
- Brasington, J., Rumsby, B. T., McVey, R. A., 2000. Monitoring and modelling morphological change in a braided gravel-bed river using high resolution GPS-based survey. *Earth Surface Processes and Landforms* 25 (9), 973–990.
- Calderón, R., Montes-Borrego, M., Landa, B. B., Navas-Cortés, J. A., Zarco-Tejada, P. J., 2014. Detection of downy mildew of opium poppy using high-resolution multi-spectral and thermal imagery acquired with an unmanned aerial vehicle. *Precision Agriculture* 15 (6), 639–661.
- Carrivick, J., Smith, M., J. Quincey, D., 2016. Structure from Motion in the Geosciences.

- Chandler, J., 1999. Effective application of automated digital photogrammetry for geomorphological research. *Earth Surface Processes and Landforms* 24 (1), 51–63.
- Colomina, I., Molina, P., 2014. Unmanned aerial systems for photogrammetry and remote sensing: A review. *ISPRS Journal of Photogrammetry and Remote Sensing* 92, 79 – 97.
- Deng, L., Mao, Z., Li, X., Hu, Z., Duan, F., Yan, Y., 2018. UAV-based multispectral remote sensing for precision agriculture: A comparison between different cameras. *ISPRS Journal of Photogrammetry and Remote Sensing* 146, 124–136.
- Dustin, M. C., 2015. Monitoring Parks With Inexpensive UAVs: Cost Benefits Analysis For Monitoring And Maintaining Parks Facilities. Ph.D. thesis, University of Southern California.
- Eisenbeiß, H., Zurich, E. T. H., Eisenbeiß, H., Zürich, E. T. H., 2009. UAV photogrammetry. Ph.D. thesis.
- Fahlstrom, P. G., Gleason, T. J., 2012. *Introduction to UAV Systems*, Fourth Edition. John Wiley & Sons, Ltd.
- Federal Aviation Administration, 2016a. No Drone Zone.  
[https://www.faa.gov/uas/resources/community\\_engagement/no\\_drone\\_zone/](https://www.faa.gov/uas/resources/community_engagement/no_drone_zone/)
- Federal Aviation Administration, 2016b. Part 107 Waivers.  
[https://www.faa.gov/uas/commercial\\_operators/part\\_107\\_waivers/](https://www.faa.gov/uas/commercial_operators/part_107_waivers/)
- Federal Aviation Administration, 2016c. Summary of Small Unmanned Aircraft Rule (Part 107).  
[https://www.faa.gov/uas/media/part\\_107\\_summary.pdf](https://www.faa.gov/uas/media/part_107_summary.pdf)
- Federal Aviation Administration, 2018. Integration of Civil Unmanned Aircraft Systems (UAS) in the National Airspace System (NAS) Roadmap Federal Aviation Administration Second Edition. Tech. rep.  
[https://www.faa.gov/uas/resources/policy\\_library/media/Second\\_Edition\\_Integration\\_of\\_Civil\\_UAS\\_NAS\\_Roadmap\\_July%202018.pdf](https://www.faa.gov/uas/resources/policy_library/media/Second_Edition_Integration_of_Civil_UAS_NAS_Roadmap_July%202018.pdf)
- Fitzpatrick, B. P., 2015. Unmanned Aerial Systems for Surveying And Mapping: Cost Comparison of UAS versus Traditional Methods of Data Acquisition. Ph.D. thesis, University of Southern California.
- Fonstad, M. A., Dietrich, J. T., Courville, B. C., Jensen, J. L., Carbonneau, P. E., 2013. Topographic structure from motion: a new development in photogrammetric measurement. *Earth Surface Processes and Landforms* 38 (4), 421–430.
- Gomez, C., Hayakawa, Y., Obanawa, H., 2015. A study of japanese landscapes using structure from motion derived DSMs and DEMs based on historical aerial photographs: New opportunities for vegetation monitoring and diachronic geomorphology. *Geomorphology* 242, 11–20.
- Gonzalez-Dugo, V., Zarco-Tejada, P., Nicolás, E., Nortes, P. A., Alarcón, J. J., Intrigliolo, D. S., Fereres, E., 2013. Using high resolution UAV thermal imagery to assess the variability in the water status of five fruit tree species within a commercial orchard. *Precision Agriculture* 14 (6), 660–678.

- Gray, P., Ridge, J., Poulin, S., Seymour, A., Schwantes, A., Swenson, J., Johnston, D., 2018. Integrating drone imagery into high resolution satellite remote sensing assessments of estuarine environments. *Remote Sensing* 10 (8), 1257.
- Hassan-Esfahani, L., Torres-Rua, A., Jensen, A., McKee, M., 2015. Assessment of surface soil moisture using high-resolution multi-spectral imagery and artificial neural networks. *Remote Sensing* 7 (3), 2627–2646.
- Heritage, G. L., Milan, D. J., Large, A. R. G., Fuller, I. C., 2009. Influence of survey strategy and interpolation model on DEM quality. *Geomorphology* 112 (3-4), 334–344.
- Hodge, R., Brasington, J., Richards, K., 2009. Analysing laser-scanned digital terrain models of gravel bed surfaces: linking morphology to sediment transport processes and hydraulics. *Sedimentology* 56 (7), 2024–2043.
- Hogg, A. R., Holland, J., 2008. An evaluation of DEMs derived from LiDAR and photogrammetry for wetland mapping. *The Forestry Chronicle* 84 (6), 840–849.
- Hugenholtz, C., Brown, O., Walker, J., Barchyn, T., Nesbit, P., Kucharczyk, M., Myshak, S., 2016. Spatial Accuracy of UAV-Derived Orthoimagery and Topography: Comparing Photogrammetric Models Processed with Direct Geo-Referencing and Ground Control Points. *GEOMATICA* 70 (1), 21–30.
- Husson, E., Ecke, F., Reese, H., Husson, E., Ecke, F., Reese, H., 2016. Comparison of Manual Mapping and Automated Object-Based Image Analysis of Non-Submerged Aquatic Vegetation from Very-High-Resolution UAS Images. *Remote Sensing* 8 (9), 724.
- James, M. R., Robson, S., 2012. Straightforward reconstruction of 3D surfaces and topography with a camera: Accuracy and geoscience application. *Journal of Geophysical Research: Earth Surface* 117 (F3), 1–17, f03017.
- Jenson, S. K., 1991. Applications of hydrologic information automatically extracted from digital elevation models. *Hydrological Processes* 5 (1), 31–44.
- Jiang, T., Geller, J., Ni, D., Collura, J., 2016. Unmanned aircraft system traffic management: Concept of operation and system architecture. *International Journal of Transportation Science and Technology* 5 (3), 123–135.
- Johnson, K., Nissen, E., Saripalli, S., Arrowsmith, J. R., McGarey, P., Scharer, K., Williams, P., Blisniuk, K., oct 2014. Rapid mapping of ultrafine fault zone topography with structure from motion. *Geosphere* 10 (5), 969–986.
- Kenward, T., 2000. Effects of digital elevation model accuracy on hydrologic predictions. *Remote Sensing of Environment* 74 (3), 432–444.
- Khanal, S., Fulton, J., Shearer, S., 2017. An overview of current and potential applications of thermal remote sensing in precision agriculture. *Computers and Electronics in Agriculture* 139, 22–32.

- Kostrzewa, J., Meyer, W. H., Laband, S., Terre, W. A., Petrovich, P., Swanson, K., Sundra, C., Sener, W., Wilmott, J., 2003. Infrared microsensor payload for miniature unmanned aerial vehicles. In: Carapezza, E. M. (Ed.), *Unattended Ground Sensor Technologies and Applications V*. SPIE.
- Laliberte, A. S., Goforth, M. A., Steele, C. M., Rango, A., 2011. Multispectral remote sensing from unmanned aircraft: Image processing workflows and applications for rangeland environments. *Remote Sensing* 3 (11), 2529–2551.
- Lane, S. N., Richards, K. S., Chandler, J. H., 1994. Developments in monitoring and modelling small-scale river bed topography. *Earth Surface Processes and Landforms* 19 (4), 349–368.
- Lang, M., Bourgeau-Chavez, L., Tiner, R., Klemas, V., 2015. Advances in remotely sensed data and techniques for wetland mapping and monitoring. In: *Remote Sensing of Wetlands*. CRC Press, pp. 79–116.
- Li, Q. S., Wong, F. K., Fung, T., 2017. Assessing the utility of UAV-borne hyperspectral image and photogrammetry derived 3D data for wetland species distribution quick mapping. *International Archives of the Photogrammetry, Remote Sensing and Spatial Information Sciences - ISPRS Archives* 42 (2W6), 209–215.
- Liu, T., Abd-Elrahman, A., 2018. Multi-view object-based classification of wetland land covers using unmanned aircraft system images. *Remote Sensing of Environment* 216, 122–138.
- Lowe, D. G., 2004. Distinctive image features from scale-invariant keypoints. *International Journal of Computer Vision* 60 (2), 91–110.
- Madden, M., Jordan, T., Bernardes, S., Cotten, D. L., O’Hare, N., Pasqua, A., 2015. Unmanned Aerial Systems and Structure from Motion Revolutionize Wetlands Mapping. In: *Remote sensing of wetlands: Applications and advances*. No. April. pp. 195–220.
- Mahlein, A.-K., 2016. Plant disease detection by imaging sensors – parallels and specific demands for precision agriculture and plant phenotyping. *Plant Disease* 100 (2), 241–251.
- Manfreda, S., McCabe, M. F., Miller, P. E., Lucas, R., Pajuelo Madrigal, V., Mallinis, G., Ben Dor, E., Helman, D., Estes, L., Ciraolo, G., Muñillerov´a, J., Tauro, F., de Lima, M. I., de Lima, J. L. M. P., Maltese, A., Frances, F., Caylor, K., Kohv, M., Perks, M., Ruiz-P´erez, G., Su, Z., Vico, G., Toth, B., 2018. On the use of unmanned aerial systems for environmental monitoring. *Remote Sensing* 10 (4).
- Matese, A., Toscano, P., Di Gennaro, S. F., Genesio, L., Vaccari, F. P., Primicerio, J., Belli, C., Zaldei, A., Bianconi, R., Gioli, B., 2015. Intercomparison of uav, aircraft and satellite remote sensing platforms for precision viticulture. *Remote Sensing* 7 (3), 2971–2990.
- McCabe, M. F., Aragon, B., Houborg, R., Mascaro, J., 2017. CubeSats in hydrology: Ultrahigh-resolution insights into vegetation dynamics and terrestrial evaporation. *Water Resources Research* 53 (12), 10017–10024.

- Micheletti, N., Chandler, J. H., Lane, S. N., 2015. Structure from Motion (SfM) Photogrammetry. In: Cook, S.J., C. L. . N. J. (Ed.), *Geomorphological Techniques*. British Society for Geomorphology.
- Mitsch, W. J., Gosselink, J. G., 2007. *Wetlands*. Wiley.
- Nebiker, S., Lack, N., Abächerli, M., Läderach, S., 2016. Light-weight multispectral UAV sensors and their capabilities for predicting grain yield and detecting plant diseases. *ISPRS - International Archives of the Photogrammetry, Remote Sensing and Spatial Information Sciences XLI-B1*, 963–970.
- Nex, F., Remondino, F., 2014. UAV for 3d mapping applications: a review. *Applied Geomatics* 6 (1), 1–15.
- Oerke, E.-C., Fröhling, P., Steiner, U., 2010. Thermographic assessment of scab disease on apple leaves. *Precision Agriculture* 12 (5), 699–715.
- Oliensis, J., 2000. A critique of structure-from-motion algorithms. *Computer Vision and Image Understanding* 80 (2), 172–214.
- O'Shaughnessy, S. A., Evett, S. R., Colaizzi, P. D., Howell, T. A., 2012. A crop water stress index and time threshold for automatic irrigation scheduling of grain sorghum. *Agricultural Water Management* 107, 122–132.
- Osroosh, Y., Peters, R. T., Campbell, C. S., Zhang, Q., 2015. Automatic irrigation scheduling of apple trees using theoretical crop water stress index with an innovative dynamic threshold. *Computers and Electronics in Agriculture* 118, 193–203.
- Pádua, L., Vanko, J., Hruška, J., Adão, T., Sousa, J. J., Peres, E., Morais, R., mar 2017. UAS, sensors, and data processing in agroforestry: a review towards practical applications. *International Journal of Remote Sensing* 38 (8-10), 2349–2391.
- Pajares, G., apr 2015. Overview and current status of remote sensing applications based on unmanned aerial vehicles (UAVs). *Photogrammetric Engineering & Remote Sensing* 81 (4), 281–330.
- Pande-Chhetri, R., Abd-Elrahman, A., Liu, T., Morton, J., Wilhelm, V. L., 2017. Object-based classification of wetland vegetation using very high-resolution unmanned air system imagery. *European Journal of Remote Sensing* 50 (1), 564–576.
- Przybilla, H., Wester-Ebbinghaus, W., 1979. Bildflug mit ferngelenktem Kleinflugzeug. *Bildmessung und Luftbildwesen. Zeitschrift für Photogrammetrie und Fernerkundung* (47), 137–142.
- Qi, S., Wang, F., Jing, L., 2018. Unmanned aircraft system pilot/operator qualification requirements and training study. *MATEC Web of Conferences* 179, 03006.
- Remondino, F., 2011. Heritage recording and 3d modeling with photogrammetry and 3d scanning. *Remote Sensing* 3, 1104–1138.

- Sankey, T. T., McVay, J., Swetnam, T. L., McClaran, M. P., Heilman, P., Nichols, M., 2017. UAV hyperspectral and lidar data and their fusion for arid and semi-arid land vegetation monitoring. *Remote Sensing in Ecology and Conservation* 4 (1), 20–33.
- Sanz-Ablanedo, E., Chandler, J., Rodríguez-Pérez, J., Ordóñez, C., 2018. Accuracy of unmanned aerial vehicle (UAV) and SfM photogrammetry survey as a function of the number and location of ground control points used. *Remote Sensing* 10 (10), 1606.
- Seitz, S., Curless, B., Diebel, J., Scharstein, D., Szeliski, R., 2006. A comparison and evaluation of multiview stereo reconstruction algorithms. In: 2006 IEEE Computer Society Conference on Computer Vision and Pattern Recognition - Volume 1 (CVPR'06). IEEE.
- Senthilnath, J., Kandukuri, M., Dokania, A., Ramesh, K., 2017. Application of UAV imaging platform for vegetation analysis based on spectral-spatial methods. *Computers and Electronics in Agriculture* 140, 8–24.
- Shafian, S., Maas, S., 2015. Index of soil moisture using raw landsat image digital count data in texas high plains. *Remote Sensing* 7 (3), 2352–2372.
- Smith, M., Carrivick, J., Quincey, D., 2015. Structure from motion photogrammetry in physical geography. *Progress in Physical Geography: Earth and Environment* 40 (2), 247–275.
- Snavely, N., Seitz, S. M., Szeliski, R., 2007. Modeling the world from internet photo collections. *International Journal of Computer Vision* 80 (2), 189–210.
- Snyder, G. I., Sugarbaker, L. J., Jason, A. L., Maune, D. F., 2014. National requirements for improved elevation data.
- Soliman, A., Heck, R., Brenning, A., Brown, R., Miller, S., 2013. Remote sensing of soil moisture in vineyards using airborne and ground-based thermal inertia data. *Remote Sensing* 5 (8), 3729–3748.
- Strecha, C., von Hansen, W., Gool, L. V., Fua, P., Thoennessen, U., 2008. On benchmarking camera calibration and multi-view stereo for high resolution imagery. In: 2008 IEEE Conference on Computer Vision and Pattern Recognition. IEEE.
- Tammaing, A., Hugenholtz, C., Eaton, B., Lapointe, M., 2014. Hyperspatial remote sensing of channel reach morphology and hydraulic fish habitat using an unmanned aerial vehicle (UAV): A first assessment in the context of river research and management. *River Research and Applications* 31 (3), 379–391.
- Thiel, C., Schullius, C., 2017. Comparison of UAV photograph-based and airborne lidarbased point clouds over forest from a forestry application perspective. *International Journal of Remote Sensing*, 38 (8-10), 2411–2426.
- Turner, I. L., Harley, M. D., Drummond, C. D., 2016. UAVs for coastal surveying. *Coastal Engineering* 114, 19–24.

- Ullman, S., Brenner, S., 1979. The interpretation of structure from motion. *Proceedings of the Royal Society of London. Series B. Biological Sciences* 203 (1153), 405–426.
- van der Wal, T., Abma, B., Viguria, A., Prévinaire, E., Zarco-Tejada, P. J., Serruys, P., van Valkengoed, E., van der Voet, P., 2013. Fieldcopter: unmanned aerial systems for crop monitoring services. In: *Precision agriculture '13*. Wageningen Academic Publishers, Wageningen, pp. 169–175.
- Verhoeven, G., Doneus, M., Briese, C., Vermeulen, F., 2012. Mapping by matching: a computer vision-based approach to fast and accurate georeferencing of archaeological aerial photographs. *Journal of Archaeological Science* 39 (7), 2060–2070.
- Wallace, L., Lucieer, A., Malenovsk, Z., Turner, D., Vopěnka, P., 2016. Assessment of forest structure using two UAV techniques: A comparison of airborne laser scanning and structure from motion (SfM) point clouds. *Forests* 7 (3), 62.
- Wallace, L., Lucieer, A., Watson, C., Turner, D., 2012. Development of a UAV-LiDAR system with application to forest inventory. *Remote Sensing* 4 (6), 1519–1543.
- Wan, H., Wang, Q., Jiang, D., Fu, J., Yang, Y., Liu, X., 2014. Monitoring the Invasion of *Spartina alterniflora* Using Very High Resolution Unmanned Aerial Vehicle Imagery in Beihai, Guangxi (China). *The Scientific World Journal* 2014, 1–7.
- Wang, B., Shi, W., Liu, E., 2015. Robust methods for assessing the accuracy of linear interpolated DEM. *International Journal of Applied Earth Observation and Geoinformation* 34, 198–206.
- Watts, A. C., Ambrosia, V. G., Hinkley, E. A., Watts, A. C., Ambrosia, V. G., Hinkley, E. A., 2012. Unmanned Aircraft Systems in Remote Sensing and Scientific Research: Classification and Considerations of Use. *Remote Sensing* 4 (6), 1671–1692.
- Wekerle, T., Filho, J. B. P., da Costa, L. E. V. L., Trabasso, L. G., 2017. Status and trends of smallsats and their launch vehicles — an up-to-date review. *Journal of Aerospace Technology and Management* 9 (3), 269–286.
- Wenger, S. M. B., 2016. Evaluation of SfM against traditional stereophotogrammetry and lidar techniques for DSM creation in various land cover areas. Ph.D. thesis, Stellenbosch University.
- Westaway, R. M., Lane, S. N., Hicks, D. M., 2000. The development of an automated correction procedure for digital photogrammetry for the study of wide, shallow, gravel-bed rivers. *Earth Surface Processes and Landforms* 25 (2), 209–226.
- Whitehead, K., Hugenholtz, C. H., 2014. Remote sensing of the environment with small unmanned aircraft systems (UASs), part 1: a review of progress and challenges. *Journal of Unmanned Vehicle Systems* 02 (03), 69–85.
- Wigmore, O., Mark, B., McKenzie, J., Baraer, M., Lautz, L., 2019. Sub-metre mapping of surface soil moisture in proglacial valleys of the tropical andes using a multispectral unmanned aerial vehicle. *Remote Sensing of Environment* 222, 104–118.

Zarco-Tejada, P., González-Dugo, V., Berni, J., 2012. Fluorescence, temperature and narrow-band indices acquired from a uav platform for water stress detection using a micro-hyperspectral imager and a thermal camera. *Remote Sensing of Environment* 117, 322 – 337, *remote Sensing of Urban Environments*.

Zhang, C., Kovacs, J. M., 2012. The application of small unmanned aerial systems for precision agriculture: a review. *Precision Agriculture* 13 (6), 693–712.

## 9 Appendix, Synthesis Pathway: Scouting

### Overview

A straightforward, but extremely valuable, use of UAS in NCDOT's Wetland Predictive Modelling activities is in acquiring high resolution pictures/video in difficult to access locations. Often, there is a need for highly resolved and up-to-date imagery of locations that are impractical or impossible to access. For instance, it may be impractical or too time consuming to qualitatively survey a large wetland extent. Alternatively, a hard to access area that was flagged as potential wetland in WPM or other output maps may need to be visually verified. In these cases, small, consumer-grade UAS may be used to rapidly obtain the high-resolution imagery and/or videos necessary to gain confidence in site conditions.

### Hardware

The greatest flexibility and ease of flight operations will be realized when using small, rotary-wing aircraft with integrated high-resolution video cameras. Packages such as the DJI Phantom series offer an ideal low-cost option that is quick to learn, ready-to-fly out of the box, has a high quality 4K video camera, streams video to a digital display in front of the remote pilot, and has a variety of safe-flight features including obstacle avoidance. It is unlikely that scouting needs would dictate the use of sensor equipment beyond those already integrated with the platform. Flight times vary based on flight conditions, but will average 20-30 minutes. Therefore, for maximum in-field flexibility, it is recommended that several charged replacement batteries are included in the field kit.

### Flight Planning

No a priori flight planning is necessary when using small UAS for scouting purposes. However, field operations will be most effective and efficient if an accessible take-off and landing area is identified that is close to the site, and is a safe operating environment for the remote pilot.

### Flight Operations

In scouting mode, the remote pilot has the freedom to fly above or below potential tree canopy, and pursue a flight that adapts to spontaneous target acquisition. That is to say, while pre-flight objectives such as "confirm this is actually a wetland" or "identify the location of the far extent of this waterbody" may guide the overall data collection, the remote pilot is able to collect observations for additional relevant targets that were unknown prior to flight. It is recommended that the video feed from the aircraft be saved for future reference.

### Post-processing

A major advantage of scouting mode operations for UAS is that no post-processing operations are required to obtain useful data. The result of a scouting mode data collection effort will exist in the remote pilot's notes, and in the saved flight video that may be reviewed to obtain additional information.

Regulatory Notes

Scouting missions are subject to the same regulations as any other civilian use UAS operation (see Review subsec. 4.4). The key component for the effectiveness is the use of EVLOS (Extended Visual Line of Sight, see Review fig. 18) while performing scouting of larger areas.

### **Expected Accuracy**

The accuracy of data obtained in a UAS scouting mission is typically limited not by properties of the sensor, aircraft, or data post-processing, but in the skill of the remote pilot and other interpreters.

## 10 Appendix, Synthesis Pathway: DSM and Orthophoto Generation

### Overview

The challenge in mapping wetlands lies in their delineation from the ground (see Review p. 5-7, section 2). The ability of UAS to provide sub-inch resolution imagery provide alternative solution for wetland mapping. In this Synthesis Pathway, we present the workflow for surveying and mapping areas indicating the presence of wetlands. This document is a created as a reference manual for successful acquisition of UAS data for implementation for mapping needs of WPM. First, the general steps for flight planning are outlined, followed by two case studies (Lake Wheeler and Kinston) are taken under scrutiny.

- A. **Lake Wheeler field** in Raleigh, where UAS operations are conducted for years, as an example of smooth and well established UAS procedures
- B. **Kinston Corridor** mapping example.  
NCDOT Wetland Predictive Modelling has been implemented in Lenoir County, NC for estimating wetland extent in Kinston corridor. Morgan Weatherford has provided the modeling delineation results. From dozens of prospective wetlands areas we have excluded those indicating the wetland presence on the satellite imagery and chosen an example with questionable wetland presence to test the ability of UAS mapping in providing reliable information supporting the WPM.

### General flight planning steps

There are two main parts to successful data collection for drone mapping: Planning and Flight. It is crucial to start planning the flight before you get to the field.

#### *In Advance:*

1. **Identify the Survey Area.**  
Locate on the map your target area. Check the road access and property status. Evaluate the possibility of executing a safe flight within the area of interest. Check is there are any obstacles – buildings, power lines. Google satellite view or any other current orthophoto can be used for that purpose
2. **Evaluate airspace.**
3. **Check the location** of your flight with AIRMAP.IO or chart the location on a printed aeronautical chart. Be sure the location does not fall within a restricted or “do not fly” zone.
4. **Create a flight plan:** Launch the flight planning app. Some manufactures provide the flight planning app with the purchase of the UAS that is fully compatible with the system (in the case studies it is emotion3 by senseFly), but there are many open source and proprietary solutions, mostly in the form of phone/tablet apps. The main feature of the UAS mapping software is the ability to calculate the geometric flight parameters (overlap vs. altitude vs. flight time vs. GSD) based on the area boundary

**TIP:**  
Consistent overlap leads to consistent GSD and higher quality map processing results.

**TIP:**

Store your batteries in the room temperature. Exposing them to cold temperature (for example in transport) drains their power.

**TIP:**

If you won't have access to the Internet in the field, download the background maps for your area into the flight planning app.

drawn by the user. The geometric parameters can be modified by the user. 60%-80% in overlap is recommended for mapping missions. Since the highest legal flying altitude is 400ft AGL, and GSD of the flight at that altitude can reach even 1inch/px (depending on the camera), we advise to perform mapping flights at the highest possible altitude, in order to capture the largest possible area in one flight. Before the flight, you can experiment with different flight settings and create a preliminary boundary for your mapping mission.

**Shortly Before the Flight:**

1. **Check airspace map again.** Check for NOTAMs and TFRs flight restrictions [at the FAA's web site](#). Special restrictions and temporary no-fly zones may be created for [major sports events, air shows or political events](#)
2. **Check the weather.** If it's raining, snowing, foggy, or very cold, you may have to reschedule for another day.

**In the Field:**

1. **Evaluate the area:** Check for obstructions, hazards and obstacles, like power lines, and trees or buildings that could obstruct your ability to maintain visual line of sight. Keep a safe distance from active highways to prevent accidentally flying too close to traffic.
2. **Set the boundaries:** Launch your flight planning app. Adjust your previously created plan, take into account the conditions you were evaluating in point 1
3. **Check the wind conditions.** You will need to take the wind direction into consideration in case your aircraft might drift where you don't want it (eg. trees). Check the treetops for the tell-tale signs of higher winds at tree top level. Use an portable anemometer to check and log the wind speed and direction. Be aware that changes in wind conditions can also appear between buildings (eg: condos) or over water.

**Hardware**

As indicated in the Review section 3, fixed wing aircraft have a distinct advantage for wetland mapping because their substantially higher endurance affords the ability to cover much large areas than the average multi-rotor UAS. In both: example A and B the mapping



Figure 14: eBee X. Image courtesy of SenseFly

areas are small enough to be surveyed by a rotary wing UAS, but since the efficiency of the fixed wing UAS with RTK/PPK functionality (see Review section 4.1.2., p. 23-27, especially fig. 13) is advantageous in mapping without setting the GCPs, this approach will be taken into further consideration. It is worth mentioning, that most of the mapping workflow applies to the rotary wing UAS as well hence it can be implemented to fulfill the missions. As an innovative mapping solution, we propose to use [eBee X](#) UAS produced by senseFly (which whom the NCSU has the MOA) equipped with the [S.O.D.A. 3D camera](#). (It is also possible to deploy the eBee X with the multispectral or thermal sensor).

## Flight Planning

Flight planning for fixed wing eBee X missions has been performed in [emotion3 software](#).

### Location A: Lake Wheeler Field

An example of mission plan for mapping purposes is shown on the figure below.

Flight is estimated to be 18 min long, cover almost 30 ha and estimated accuracy of the orthophoto is 2.8 cm (1.1 inch) at the maximum legal altitude of 400 ft. Since similar flights have been conducted by our research team, we have achieved resolution after the processing of 2.5 cm/ pix (see the processing report in the appendix).

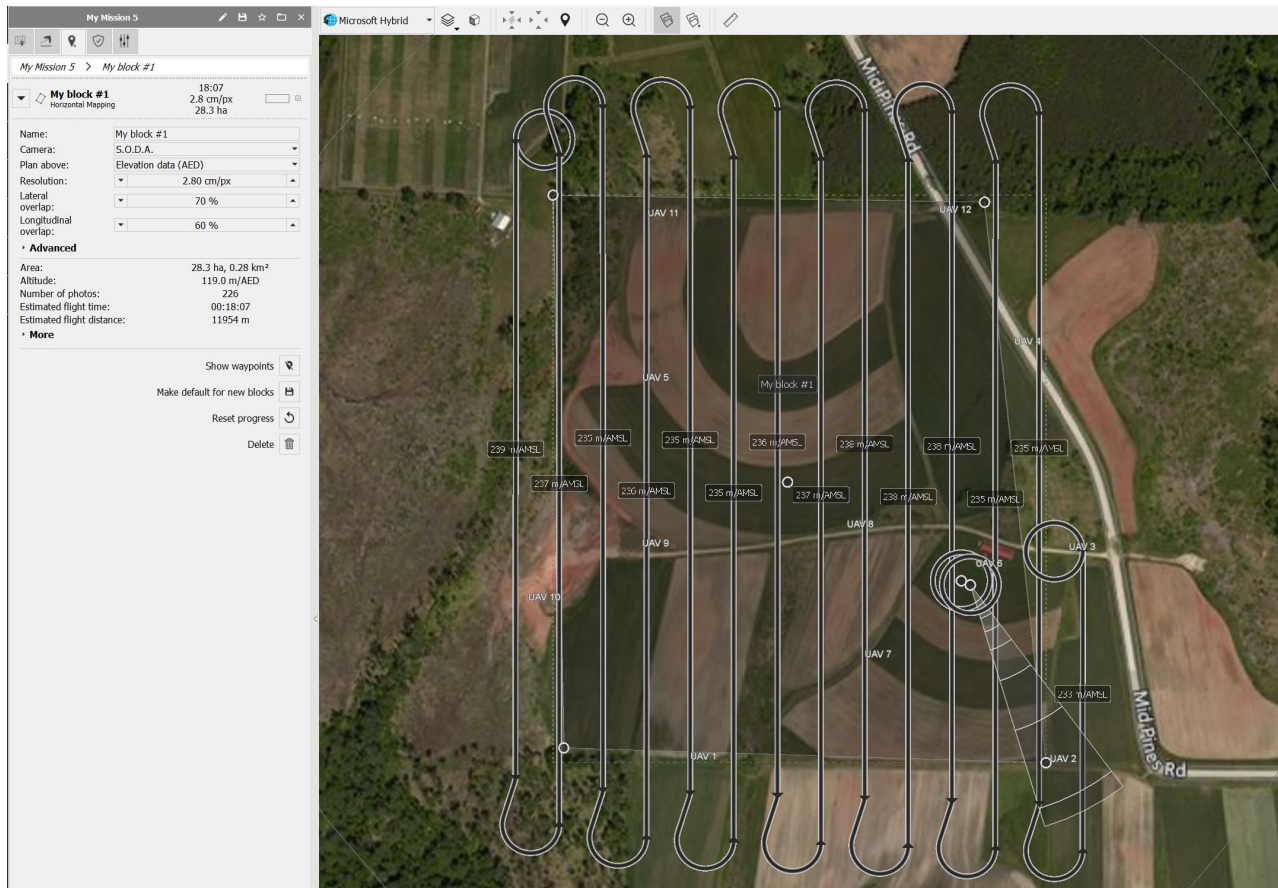


Figure 15: Flight Planning for the A location (Lake Wheeler Field), screenshot from the emotion3 software.



eBee X is hand launched and performs belly landing. The safety areas for safe take off and landing need to be free of obstructions.  
In case of operating in RTK/PPK mode, no Ground Control Points will be used during flight.

## Post-processing

Processing of the RGB imagery is described in Review section 4.2. We recommend use of the user intuitive solutions for first time use. Pix4Dmapper and Agisoft Metashape (formerly Photoscan). Both provide free trial licences and Metashape has a functionality of operation in DEMO mode. Our team is ready to deliver in person hands-on instructions for processing. The exemplary processing report is provided as an appendix.

The products of the processing include: orthophoto (expected resolution ~1 inch/pix), Digital Surface Model (expected resolution ~4 inch/pix), point cloud and 3D model (mesh).  
In case of operating in RTK/PPK mode, no Ground Control Points will be used in imagery processing.

## Regulatory Notes

We are able to operate under part 107 (see Review section 4.4.). Since the mapping areas do not have large extent, the line of sight will be able to be maintained under good weather conditions. Both flights will be conducted below or at the legal altitude limit (400 ft ASL). Since the procedures for the Lake Wheeler location are well established, the main focus would be to research the location B. As visible on the aeronautical chart (Fig 6), the area is within class G airspace. The access is possible through a public road and the flight is designed to avoid residential areas (see Fig 4 and 5). The information about the parcels above which the flight will be conducted has been gathered: all are private property classified as either woodland or agricultural use.

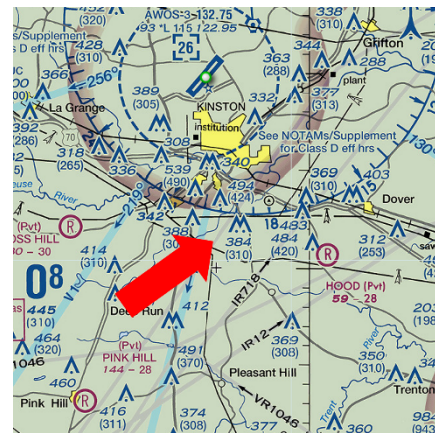


Figure 18: Fragment of the aeronautical chart. The arrow points at the flight area.

## 11 Appendix, Synthesis Pathway: LiDAR

### Overview

A wide variety of LiDAR sensors designed for small UAS deployment have recently become available to consumers. Along with RTK positioning hardware and software, these LiDAR instruments have great potential for NCDOT applications; including, but certainly not limited to wetland mapping activities. Compared to other sensing modalities, the primary advantage of LiDAR is the ability to estimate structure in the vertical dimension with extreme accuracy. Compared to the digital *surface* models that can be created with standard cameras and SFM software, most LiDAR instruments offer the potential to create both surface models *and* “bare Earth” digital elevation models. This is because most LiDAR instruments can record multiple “return” signals from a single laser pulse. The first return may indicate the position of the top of the forest canopy whereas subsequent returns reveal information about successively deeper layers of the surface structure, including the ground. This is of particular interest for detailed wetland predictive modeling in areas with significant vegetation canopy. In fact, with the exception of *possibly* mapping hydrophytic species presence using hyperspectral imagery, we are aware of no other method capable of mapping likely wetland locations under closed forest canopy. However, UAS-LiDAR systems and associated post-processing are currently more complicated than alternative UAS sensing technologies. Precise aircraft positioning is essential for acquiring good data, so RTK GNSS techniques are required. Sensor-platform integration is also less turn-key than many alternative solutions, although there is a growing number of fully-integrated options.

### Hardware

Table 8 in our primary review document highlights several of the currently available small UAS mountable LiDAR systems. Note that this marketplace is moving as fast or faster than the rest of the UAS market. When selecting a LiDAR sensor for UAS deployment, a few factors are paramount: weight, power (range), number of returns recorded, scan range, and accuracy. Available LiDARs range in weight from <1 kg to nearly 4 kg. While most medium to large consumer-class UAS can carry these instruments, there will be substantial tradeoffs in flight endurance. Instrument miniaturization necessitates sacrifices in laser power, which reduces the effective range of these small LiDARs in comparison to their aircraft-mounted counterparts. With few exceptions, these instruments must be flown around 50-100 m from the ground. The number of returns recorded by a LiDAR system limits what can be done with the data. The simplest systems record only the first and last return, whereas “full waveform” instruments capture return information continuously. We believe that simple first/last return systems are fully capable of supplying data useful for wetland predictive modeling. The scan range for a system describes the angles through which the instrument can collect data. Ranges vary from less than 45 degrees to 360 degrees, in both side-to-side and front-to-back directions. Accuracy typically decreases with scan angle, so it is recommended that data be filtered to points taken within 45 degrees of nadir. Therefore, any system covering at least 90 degrees of scan angle will be fully capable. Specifications such as sampling frequency also affect the collected data, but most available systems have sampling frequencies in excess of what is required for accurate

mapping. That is, most systems can provide several hundred points per square meter at typical flight speeds and altitudes. While this point density is overkill in many contexts, exceptionally high point densities are required when the goal is to retrieve bare earth points under dense vegetated canopy. In these cases, the vast majority of points will be intercepted by leaves and branches and very few will find their way through, and back out, of canopy gaps.

LiDAR systems will publish absolute accuracies which describe their ability to measure a distance. These are typically 1-5 cm. However, in a LiDAR-UAS context, the accuracy of the platforms inertial measurement unit (IMU) and geographic positioning system usually are the larger limit on accuracy. In short, while the onboard RTK enabled GNSS positioning systems found on most current aircraft can provide sub-centimeter x,y,z locational accuracy, the onboard IMU (which measures the orientation of the platform) often does not deliver high enough accuracy for LiDAR data acquisition, although it is good enough for aircraft navigation. Many new LiDAR systems designed for UAS have integrated IMU systems that sidestep this issue (e.g. the Phoenix Scout and Ranger series).

## **Flight Planning**

The first step in flight planning for UAS LiDAR data acquisition is the determination of the required point density. This density, in conjunction with the sensor's sampling frequency and scan width, will dictate flight speed and altitude, which will determine the swath width, and consequently the number of flight lines necessary to cover the study area. As previously mentioned point densities in excess of 400 points per square meter are usually necessary to ensure sufficient bare ground samples. Flight parameters necessary to achieve these densities depend on the particular sensor's sampling frequency and scan angle, but most systems can achieve this with flight speeds in the 8-10 m/s range and at altitudes of 50-100 m. Luckily, many of the leading suppliers of UAS LiDAR instruments have standalone or online software that will aid in this flight planning process.

## **Flight Operations**

In most ways, flight operations for LiDAR data acquisition are identical to other sensing modalities. Once the flight has been planned, usually with the assistance of vendor-supplied software, the flight plan details are uploaded to the aircraft. The aircraft will then fly autonomously according to this flight plan, with the possible exception of takeoff and landing. Some LiDAR sensor packages (e.g. Phoenix Scout) offer the ability to visualize the data in real time. This is a great advantage because the real time view can help to diagnose flight planning problems that are resulting in suboptimal data. For example, perhaps the chosen point density is insufficient due to vegetation coverage in the field. Additionally, it is essential that RTK base stations be deployed appropriately, either to correct GNSS positions in real-time, or through post-processing. UAS LiDAR data acquisitions from uncorrected GNSS positions are likely of little value.

## **Post-processing**

Any LiDAR data acquisition will result in millions of data points recording the x,y,z (and possibly intensity) values for one or more laser pulse returns. These data can be used to create a wide variety of final products, but bare earth digital elevation models are the most relevant for wetland predictive modeling applications. This process relies on software to separate ground returns from all others. Once separated, it is usually necessary to interpolate elevation values between these points in order to create a continuous surface. At that point, the resulting bare earth digital elevation model may be exported at a spatial resolution dictated by the project, and geolocated on Earth.

## **Regulatory Notes**

There are no legal differences between a UAS with and without LiDAR. A major regulatory constraint is the need of the aircraft to be in line of sight at all times during the flight (see Review subsec. 4.4). Another significant barrier preventing UAS from replacing the airborne LiDAR surveys is the limitation of 55 lbs. weight (with a payload) for civilian UAS use. Many high grade LiDAR sensors are heavy and require a high payload capacity carrier. This can frequently reach weights exceeding the legal limits. The tradeoffs between LiDAR sensor quality and its weight need to be balanced. An example of a LiDAR equipped UAS that doesn't exceed the legal weight limit is the [Delair DT26X LiDAR](#) (ca. \$300,000), weighing 37.5 lbs. and carrying a 15 mm accuracy LiDAR (at 400 ft, flying altitude which is the legal flight ceiling).

## **Expected Accuracy**

The accuracy (in this case the fidelity of measurements of surface elevation) is determined in large part by the LiDAR sensor itself, the GNSS accuracy, and the IMU accuracy. While many high-end LiDAR sensors boast absolute accuracies of a few centimeters, it is likely that the combination of sensor, location, and IMU accuracies will result in elevation values that deviate by at least several centimeters from reality.